ANNUAL REVIEWS

Annual Review of Earth and Planetary Sciences

On Dislocation Climb as an Important Deformation Mechanism for Planetary Interiors

Philippe Carrez,[1] Alexandre Mussi,[1] and Patrick Cordier[1,2]

[1]Université de Lille, CNRS, INRAE, Centrale Lille, UMR 8207 - UMET - Unité Matériaux et Transformations, Lille, France; email: Patrick.Cordier@univ-lille.fr

[2]Institut Universitaire de France, Paris, France

Annu. Rev. Earth Planet. Sci. 2024. 52:409–41

First published as a Review in Advance on January 18, 2024

The *Annual Review of Earth and Planetary Sciences* is online at earth.annualreviews.org

https://doi.org/10.1146/annurev-earth-031621-063108

Keywords

creep, dislocation climb, diffusion, mantle convection

Abstract

An understanding of the rheological behavior of the solid Earth is fundamental to provide a quantitative description of most geological and geophysical phenomena. The continuum mechanics approach to describing large-scale phenomena needs to be informed by a description of the mechanisms operating at the atomic scale. These involve crystal defects, mainly vacancies and dislocations. This often leads to a binary view of creep reduced to diffusion creep or dislocation creep. However, the interaction between these two types of defects leading to dislocation climb plays an important role, and may even be the main one, in the high-temperature, low strain rate creep mechanisms of interest to the Earth sciences. Here we review the fundamentals of dislocation climb, highlighting the specific problems of minerals. We discuss the importance of computer simulations, informed by experiments, for accurately modeling climb. We show how dislocation climb increasingly appears as a deformation mechanism in its own right. We review the contribution of this mechanism to mineral deformation, particularly in Earth's mantle. Finally, we discuss progress and challenges, and we outline future work directions.

- Dislocations can be sources or sinks of vacancies, resulting in a displacement out of the glide plane: climb.

- Dislocation climb can be a recovery mechanism during dislocation creep but also a strain-producing mechanism.
- The slow natural strain rates promote the contribution of climb, which is controlled by diffusion.
- In planetary interiors where dislocation glide can be inhibited by pressure, dislocation climb may be the only active mechanism.

1. INTRODUCTION

When Reiner and Bingham established rheology as a branch of science designed to study the way matter flows, they introduced a dimensionless number called the Deborah number (Reiner 1964). Depending on the ratio between the time of observation and a characteristic time of the material (a so-called relaxation time), it would behave as a solid or flow as a liquid. The biblical reference to Deborah comes from a verse in the Book of Judges, "The mountains flowed before the Lord," which can be interpreted as a statement that, as Heraclitus would later say, "everything flows" given enough time. However, understanding Earth's slow deformations on a human scale is no easy task, and, as an example, Wegener is known to have struggled with the difficulty of describing the causal forces and mechanisms involved in continental drift. The concept of crystalline defects, which emerged in the early twentieth century, now makes it possible to describe how crystalline matter and rocks in particular deform. A distinction is made between dislocations, linear defects that contribute to thermally activated creep, highly sensitive to the applied stress, and vacancies, point defects present at high temperatures and involved in creep whose efficiency is highly dependent on grain size. Dislocation creep, which generates crystal preferred orientations (CPOs), is considered a major mode of deformation in the lithosphere and upper mantle, whereas diffusion creep (which does not produce CPOs) was spontaneously considered more relevant to the rheology of the lower mantle. However, new experimental (high-pressure deformation) and theoretical (multiscale numerical modeling) approaches have led us to question this vision, which was based on few direct observations. Indeed, there is another mechanism in which these two types of crystal defects play a cooperative role: dislocation climb. A creep mechanism was proposed very early on based on dislocation climb (Nabarro 1967b) but was hardly ever considered in the rheology of Earth materials, especially in the last 20 years. As we shall show, recent results suggest not only its (ubiquitous) activity in mineral deformation but also that in planetary interiors, it may even be the only operative mechanism (see the sidebar titled Unlocking Rock Deformation: Mechanisms Matter).

The aims of this article are to review the fundamentals of the field, to highlight recent developments in both observations and numerical modeling approaches, and to underline the lines of further research required. We first summarize the basic concepts, both on the basis of historical proposals and in light of recent modeling approaches. We then show how climb has evolved from essentially a recovery mechanism into a deformation mechanism in its own right. We then discuss why we think this trend should be even more critical for the deformation of planetary interiors. Finally, we highlight the challenges and difficulties that will condition future research.

2. DISLOCATION MOTION: GLIDE VERSUS CLIMB

Dislocations are among the main carriers of deformation in crystal plasticity. These linear defects are characterized locally by two vectors: the line vector $\vec{u}$ and the Burgers vector $\vec{b}$, which describes

UNLOCKING ROCK DEFORMATION: MECHANISMS MATTER

The science of rock deformation is complex because it is a property that depends on physical conditions (pressure, temperature), environmental conditions (e.g., oxygen fugacity for certain minerals or activity of other phases), and microstructural parameters (e.g., grain size). It is also a behavioral property that describes the material's response to a given type of solicitation. In geodynamics, we are particularly interested in stationary creep, i.e., the strain rate resulting from the application of a constant stress, but other modes of solicitation can also be considered, such as the anelasticity involved in intrinsic seismic attenuation. This complexity was addressed by Ashby (1972), who proposed the construction of maps describing, in a given parameter field, the type of deformation (diffusion creep, dislocation creep, grain boundary sliding) that supplies the greater strain rate. The large number of parameters (not always well known, such as microstructural parameters) potentially involved makes the construction of these maps a complex task. The major difficulty, however, remains the need to extrapolate experimental data to the very slow strain rates of Earth dynamics. However, the deformation modes shown in these maps often involve several microscopic mechanisms, each with its own strain rate dependence, which makes extrapolation so challenging. That is why we are convinced that it is necessary to push the description to the scale of elementary mechanisms such as dislocation climb, which is the subject of this review.

the discontinuity of the lattice induced by the defect. When $\vec{u}$ and $\vec{b}$ are parallel, the dislocation is called screw. It can geometrically move by glide in any plane. In any other case, the dislocation exhibits an edge component (the pure edge dislocation corresponds to the case where $\vec{u}$ and $\vec{b}$ are perpendicular) and its conservative motion is restricted to the plane defined by $\vec{u}$ and $\vec{b}$ (the so-called glide plane) (**Figure 1*a***). This mode of displacement called glide results from the application of a stress and produces plastic strain. The combination of the shear direction characterized by the Burgers vector $\vec{b}$ and the plane in which the dislocations glide defines the so-called slip system. A slip system is generally expressed in crystallographic notation [uvw](hkl), with [uvw] being the direction parallel to $\vec{b}$ and (hkl) representing the glide plane. Depending on crystal symmetry, there may be several equivalent slip systems, in which case we refer to the family of equivalent slip systems noted <uvw>{hkl}. When a vacancy diffuses toward an edge dislocation line and is absorbed (or the other way around is emitted), a short segment of the dislocation line moves away from the glide plane in a plane perpendicular to the Burgers vector, producing a jog (Mott 1951). This nonconservative process, called climb (**Figure 1*b***), is the focus of this review. It also responds to the application of a stress but depends very strongly on the presence of vacancies and their ability to move toward the dislocations.

From a kinematic point of view, let us consider a dislocation $\vec{b}$ moving (either by glide or by climb) in a plane $\vec{n}$ ($\vec{n}$ is the unit vector normal to the plane). The Schmid tensor obtained from the dyadic product $\vec{b} \otimes \vec{n}$ can be decomposed into symmetric and antisymmetric parts:

$$b_i n_j = \varepsilon_{ij} + \omega_{ij} = \frac{1}{2}(b_i n_j + b_j n_i) + \frac{1}{2}(b_i n_j - b_j n_i). \quad 1.$$

$\bar{\bar{\varepsilon}}$ is either the symmetric glide tensor or the symmetric climb tensor; $\bar{\bar{\omega}}$ is the plastic rotation tensor. We note that in case of climb, $\vec{b}$ and $\vec{n}$ are collinear so the distortion is a pure shear that produces no rigid-body rotation, unlike glide, which produces a simple shear. Dislocation climb therefore does not contribute to the formation of CPOs. By extension with the notion of a slip system, we can define a climb system [uvw](HKL), with [uvw] (still parallel to $\vec{b}$) perpendicular to (HKL).

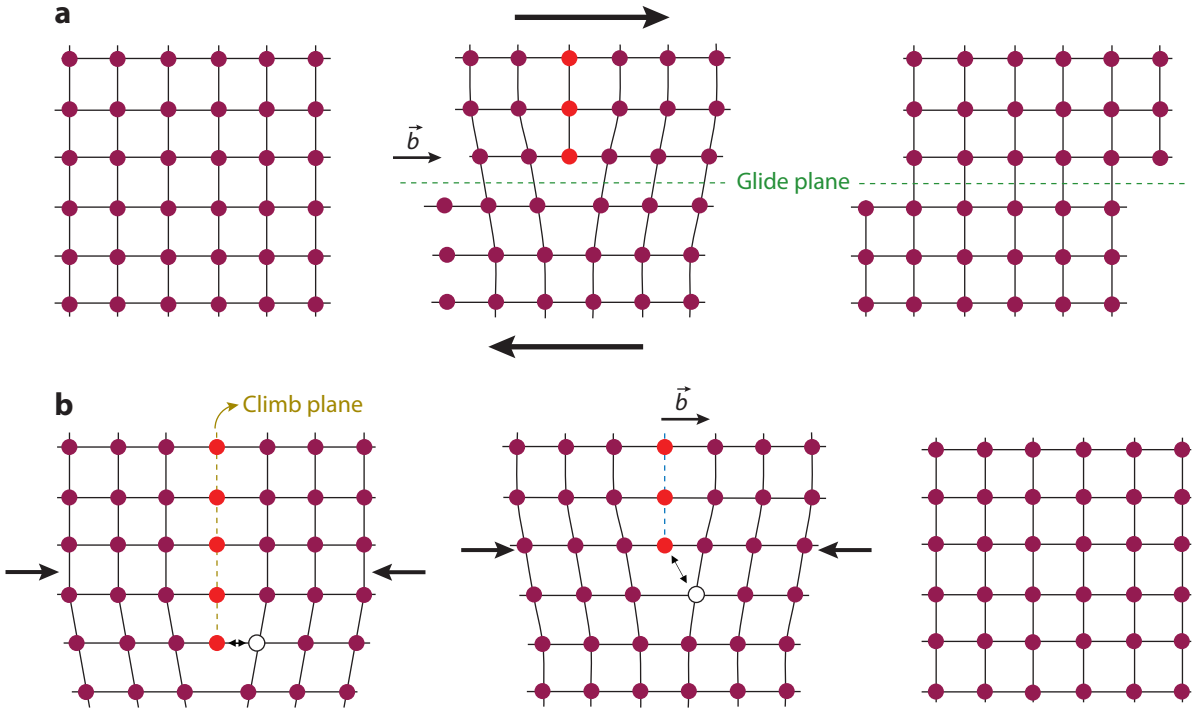

Figure 1

An edge dislocation characterized by a Burgers vector $\vec{b}$ and a line perpendicular to the plane of representation moves by (*a*) glide under a shear stress and (*b*) climb under a lateral compressive stress. Here the empty symbol represents a vacancy, which diffuses to the core to promote climb motion.

3. DISLOCATIONS AS SINKS (OR SOURCES) FOR VACANCIES

3.1. Observations

Because climb occurs when a dislocation absorbs or emits a vacancy, the role of dislocations as sources or sinks of vacancies is first considered. It is also through this mechanism that some features of climb were first revealed. Indeed, the equilibrium vacancy concentration increases dramatically with increasing temperature, and materials quenched rapidly from high temperature can be strongly supersaturated in vacancies. Annealing at moderate temperature (which corresponds to a lower equilibrium concentration but high enough that diffusion occurs) leads to the elimination of vacancies by absorption at sinks. Grain boundaries can potentially play the role of sources or sinks for point defects. However, for grain boundaries being able to maintain the vacancies at thermodynamic equilibrium, it is necessary to have a grain size smaller than the distances over which diffusion takes place. Otherwise, additional sources and sinks must be found inside the grains. Early observations of very peculiar dislocation microstructures have shown that dislocations can play the role of sinks (**Figure 2**).

When vacancy precipitation occurs on dislocations with orientations very close to the screw orientation, their absorption leads to very unusual helical shapes (**Figure 2*a*,*b***). More generally, quenched-in vacancies precipitate into discs of vacancies that, by collapse and shear, result in prismatic dislocation loops (Hirsch et al. 1958). A very important observation is that absorption of point defects can produce sources of dislocations [either concentric or spiral (see **Figure 2*c*,*d***)]

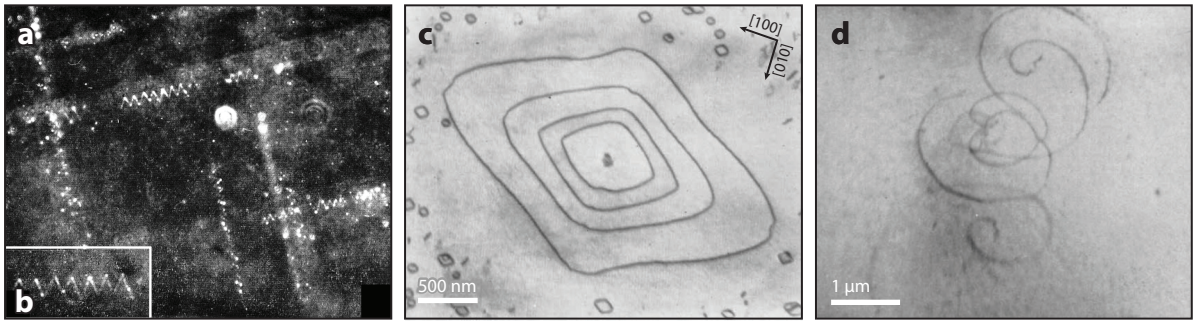

Figure 2

(*a*) Helical dislocations in NaCl formed because of the precipitation of vacancies at an almost pure screw dislocation during cooling from the melt. Magnification 600×. Panel adapted with permission from Amelinckx et al. (1957). (*b*) Helix in NaCl as in panel *a* but at a higher magnification (1,200×). Note the sharply cut angles of the projected helix suggesting a polygonal shape of the helix. (*c*) Concentric loops formed by climb in Al-3.5%Mg quenched from 550°C in silicone oil. Panel adapted with permission from Westmacott et al. (1962). (*d*) Four [0001] dislocation climb spiral sources in magnesium quenched from 400°C, then annealed 10 min at 120°C, then quenched in liquid helium, and finally annealed 30 min at 270°C. Panel adapted with permission from Edelin & Levy (1973).

generated by climb as proposed by Seitz (1950) and Bardeen & Herring (1952) (**Figure 3**). Nowadays, the activation of Bardeen-Herring sources represents one of the major test cases in any attempt at incorporating climb processes into 3D dislocation dynamics (DD) simulations (e.g., Mordehai et al. 2008, Gao et al. 2011) (see **Figure 3**).

Condensation of point defects into dislocation loops is only the first stage of evolution of these materials under nonequilibrium conditions. Under further annealing, loops coarsen: Large loops grow at the expense of smaller ones. Several mechanisms can be involved. Large loops may grow by absorbing vacancies emitted by the shrinking loops. Coarsening is then controlled by vacancy bulk diffusion. This has been used to measure diffusion coefficients in some materials (e.g., Silcox & Whelan 1960, Chien & Heuer 1996). Coarsening can also be mediated by motion of the loops (Bakó et al. 2011) by translation in their habit plane by conservative climb (or

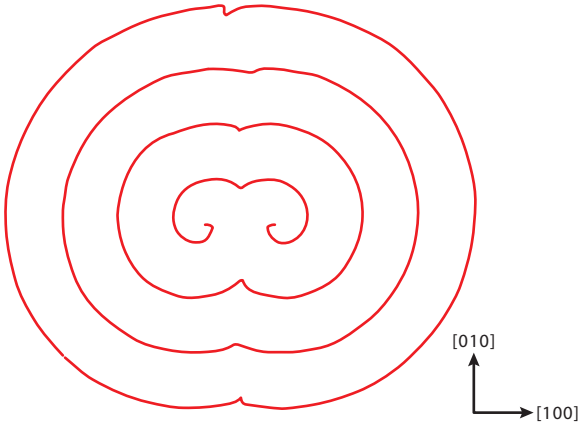

Figure 3

Development of a Bardeen-Herring source modeled with 3D discrete dislocation dynamics by Gao et al. (2011). The dislocation segment direction is [100], and the Burgers vector is [001]. The applied stress on the Bardeen-Herring source is along [001] direction, the climb plane is (001), and the climb direction is [010].

self-climb)—displacement results from transport of matter around the loop by pipe diffusion along the dislocation line—or by glide along the cylinder defined by the loop and the Burgers vector (Tisone et al. 1968). Interactions between growing noncoplanar loops can result in 3D dislocation structures (Tisone et al. 1968).

3.2. Driving Forces

The fact that dislocations play the role of sources or sinks raises the question of the interaction between them and point defects. In diffusion creep, flow of vacancies arises from heterogeneities of local equilibrium vacancy concentration in the vicinity of stressed boundaries. Similarly, here we investigate the local equilibrium vacancy concentration in the vicinity of a climbing dislocation. The free energy change associated with the creation or absorption of vacancies due to the climb of the dislocation balances the resulting plastic work. The problem is usually described in terms of forces that can have two distinct origins (Lothe 1960, Friedel 1964), elastic and osmotic, due to the supersaturation of vacancies (or interstitial atoms, a case that is equivalent but that is not discussed here). If the defect concentration c in the vicinity of the dislocation differs from the equilibrium value c_0 at that temperature, a force, called the osmotic or chemical force, will act on the dislocation line, normal to the slip plane:

$$f_o = \frac{kTb}{\Omega} \ln \frac{c}{c_0}, \tag{2.}$$

where f_o is the osmotic force per unit length, k is the Boltzmann constant, T is the temperature, b is the modulus of the Burgers vector, and Ω is the volume change due to the formation of a vacancy ($\Omega \sim b^3$). For a mixed dislocation, the osmotic force is

$$f_o = \frac{kTb_e}{\Omega} \ln \frac{c}{c_0}, \tag{3.}$$

where b_e is the edge component of the Burgers vector.

Conversely, the thermal equilibrium concentration of defect c in the vicinity of a dislocation line subject to an elastic force f_{el} is

$$c = c_0 \exp\left(\frac{-f_{el}\Omega}{bkT}\right). \tag{4.}$$

The elastic force can result from the applied stress or from the dislocation itself if its line is curved (the line tension τ). In case of loops resulting from the condensation of point defects in the absence of applied stress, the elastic force due to the line tension of the curved dislocation loop segments (curvature $1/R$) is

$$f_{el} = f_\tau = \frac{\tau}{R} \cong \frac{\mu b^2}{R}, \tag{5.}$$

where μ is the shear modulus. A Bardeen-Herring source of length L is expected to operate if the concentration of vacancies is sufficient to cause the dislocation to climb until a semicircle of curvature $R = L/2$ is reached. The dependence is given by (Nabarro 1967a)

$$\frac{L}{b} = \frac{2\mu\Omega}{kT\ln(c/c_0)}. \tag{6.}$$

Considering the case of a straight dislocation subject to an applied stress $\bar{\bar{\sigma}}$, the elastic force to consider is the climb component f_c of the Peach-Koehler force $\overrightarrow{f_{PK}} = \vec{b}.\bar{\bar{\sigma}} \times \vec{u}$:

$$\vec{f}_c = \frac{(\vec{b}.\bar{\bar{\sigma}} \times \vec{u}).(\vec{b} \times \vec{u})}{|\vec{b} \times \vec{u}|}. \tag{7.}$$

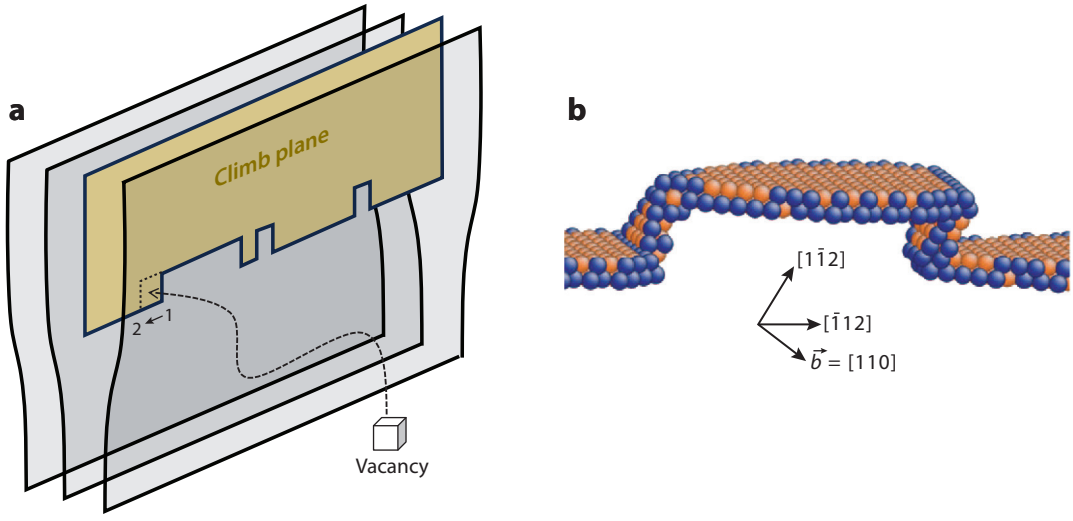

Figure 4

Jogs. (*a*) Schematic representation of jogs on the extra half-plane of an edge dislocation resulting from the absorption of vacancies. (*b*) Atomic structure of a jog pair on a dissociated edge dislocation in Cu. Dark atoms belong to the partial dislocation cores, and light ones belong to the stacking fault ribbon. Figure adapted with permission from Mordehai et al. (2008).

3.3. Climb Rate

A dislocation line cannot climb as a whole but only atom by atom, through the movement of jogs on the line (**Figure 4*a***). Jogs are the locations where emission and absorption of vacancies always take place. The climb velocity v_{cl} of the dislocation depends on the number of jogs along the line and on their drift velocity v_j. If x is the average distance between jogs, $c_j = b/x$ is the jog concentration and

$$v_{cl} = v_j c_j. \quad 8.$$

Moving a jog from 1 to 2 involves the diffusion of a vacancy away from the jog position in the bulk lattice (**Figure 4*a***). Hence, under thermal fluctuations, a jog emits or absorbs vacancies at a frequency on the order of

$$\nu_D \exp\left(\frac{-U_{sd}}{kT}\right), \quad 9.$$

where ν_D is the Debye frequency and U_{sd} is the activation energy for self-diffusion (which can be expressed in any usual energy units; note that in physics, eV is often used because the elementary processes of interest are characterized by activation energies of a few eV) (see the sidebar titled Energy: Molecular-Scale Versus Macroscopic). Under influence of a climb force f_c per unit length acting on the dislocation, the rate of emission is increased by a factor $\exp(f_c\Omega/bkT)$ and the rate of absorption is decreased by a factor $\exp(-f_c\Omega/bkT)$. As a result, the jog will drift along the dislocation line with an average velocity

$$v_j = 2\nu_D b \exp\left(\frac{-U_{sd}}{kT}\right) \sinh\left(\frac{f_c\Omega}{bkT}\right) = \frac{2D_{sd}}{b} \sinh\left(\frac{f_c\Omega}{bkT}\right) \quad 10.$$

and

$$v_{cl} = v_j c_j = \frac{2c_j D_{sd}}{b} \sinh\left(\frac{f_c\Omega}{bkT}\right), \quad 11.$$

ENERGY: MOLECULAR-SCALE VERSUS MACROSCOPIC

kT is the product of the Boltzmann constant, *k*, and the temperature, *T*. This product is used in physics as a scale factor for energy values in molecular-scale systems. In Arrhenius laws, *kT* can be assimilated to the energy supplied by thermal agitation to electrons, enabling them (or not) to cross the energy barriers involved in the studied process. In macroscopic systems, with many particles (molecules) present, *RT* might be used instead, where *R* is the molar gas constant, which is the product of the Boltzmann constant and the Avogadro constant. The SI units for *RT* are joules per mole (J/mol).

where D_{sd} is the self-diffusion coefficient. Let us consider the case where the density of jogs is very high ($c_j \approx 1$). This corresponds to the case of dislocations climbing under high temperatures and low stress and the vacancy concentration is uniform along the core:

$$v_{cl} \cong \frac{2D_{sd}}{b^2}\frac{f_c\Omega}{kT}. \quad 12.$$

The rate of climb is then determined by the rate at which vacancies can diffuse away or toward the dislocations. Thus, the activation energy for climb is close to the activation energy for bulk self-diffusion and the climb velocity scales linearly with the climb force per unit length f_c. Being thermodynamically consistent and also numerically highly efficient, this climb velocity expression represents a suitable way to introduce climb mobilities at the continuum level of DD simulations (Mordehai et al. 2008, Keralavarma et al. 2012).

However, by essence, climb dynamics involving point defects absorption or emission is a discrete process. Kabir and coworkers (2010) were able to calculate dislocation climb velocity in bcc iron by coupling molecular static calculations to a kinetic Monte Carlo (KMC) algorithm. In their approach, the diffusion path's energy landscape in the vicinity of the dislocation is calculated at the atomic scale and then transferred to the KMC to calculate the dislocation climb velocity. However, the major criticism of their study is that the whole energy landscape was not fully incorporated while the climb velocity was only accounting for vacancy absorption, disregarding the possibility of vacancy emission. Their study nevertheless showed that the climb velocity is a quantity accessible through computational modeling techniques. Along the same line, in order to capture the effect of the combination of the intrinsic discrete nature of the process, the thermal activation, and its sensitivity to elastic forces, McElfresh et al. (2021) proposed a stochastic model for simulating dislocation climb also based on a KMC scheme coupled this time to DD simulations. In this approach, KMC calculations account for a rigorous treatment of the vacancy transport kinetics while the DD simulations provide the stress field. Specifically applied to bcc iron, they show that the climb velocity naturally scales linearly with the climb force but that climb might be faster than expected from the classical treatment developed above as a consequence of the local point defects/dislocation interactions. In contrast to classical expression based on smooth point defect fluxes, recent modeling of dislocation climb tends to highlight the importance of the local point defects conditions that ultimately control the kinetics of climb. As an example, Kohnert & Capolungo (2022) have shown the heterogeneity of vacancy concentrations around dislocations using DD simulations (**Figure 5**), with some dislocations being surrounded by a vacancy-depleted region and others being in supersaturation conditions.

In case of low jog density (i.e., $C_j < 1$), the climb velocity is modified to account for the jog formation energy U_j. The corresponding formulation of v_{cl} still scales linearly with f_c, but the

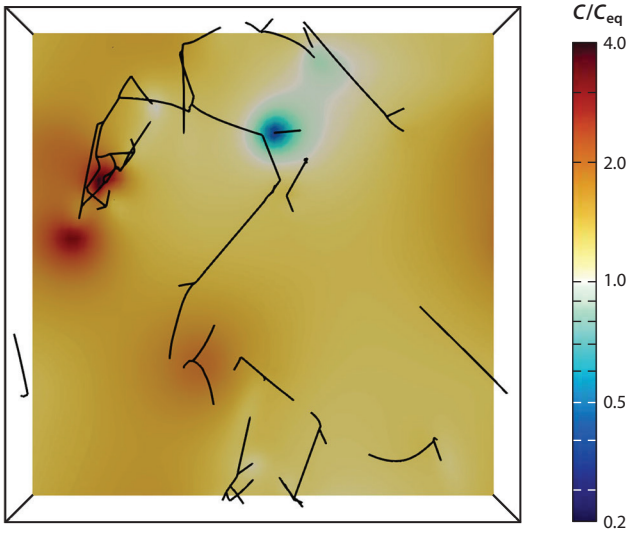

Figure 5

Vacancy distribution around a climbing dislocation network at 500°C normalized to the thermal equilibrium density C_{eq}. Climb-enabled discrete dislocation dynamics calculations from Kohnert & Capolungo (2022) with permission (CC BY 4.0).

activation energy for climb will depend on both U_{sd} and U_j (both quantities adding up). Atomistic calculations represent a promising approach to estimate U_j. Indeed, for the initiation of a jog corresponding to the binding of a vacancy to the dislocation core, its formation energy can be accurately computed at the atomic scale [as done for example in case of bcc iron by Lau et al. (2009), leading to $U_j \sim 1.7$ eV for a mixed <111>(110) dislocation]. More recently, similar calculations have been performed in MgO (Zhai et al. 2020), showing that the formation energy of a jog pair along a <110>{110} edge dislocation is 2.5 eV.

Most models, inspired by the case of metals, consider the elastic interaction between point defects and the hydrostatic stress surrounding a dislocation (with an edge component). Minerals are ionic solids, and crystal defects (point defects and dislocations) may be charged. There may be an electrostatic interaction between dislocations and point defects. These aspects have received little attention in minerals, if any. However, Hirel et al. (2016) have shown in $MgSiO_3$ bridgmanite that, even in a case where dislocations are charge neutral, there might be an interaction between charged vacancies and a dipole induced by local displacements in the core. Moreover, they showed that in bridgmanite, straight [100](010) edge dislocations favor an oxygen-deficient composition that carries a positive electric charge. The situation is likely to be more complex because climb involves jogs on the dislocation lines, which most likely carry electric charges. This has been considered only in rock salt structure and not in silicates, to the best of our knowledge.

In MgO, dislocations of Burgers vector 1/2<110> belonging to either <110>{110} or <110>{100} slip systems are neutral, but jogs that can be viewed as a piece of edge dislocation in {111} are intrinsically charged and carry a positive or negative charge half of the one of the ion (Zhai et al. 2020). As a consequence, it is unexpected to circumvent the charge carried by jogs. Because of the electric charge carried by jogs, when modeling the dislocation climb process, the jog-jog interaction or the jog-point defects interaction should be considered explicitly, Coulombic

interaction between electric charge carriers being likely to produce a bias in the diffusion of point defect in the vicinity of the dislocation line.

3.4. Pipe Diffusion and Self-Climb

The previous expressions of the climb velocity have been derived without considering the possibility that preferential diffusion (pipe diffusion) may occur along the dislocation line. Indeed, in the vicinity of dislocation cores, where the atomic arrangement can be highly distorted, the activation energy for point defect diffusion is expected to decrease substantially. As an example, in aluminum, diffusivity can be increased by three orders of magnitude along the core near 600 K (Legros et al. 2008), and the difference can be up to six orders of magnitude in bcc Fe at 700 K (Swinburne et al. 2016). Similar effects have also been documented in simple ionic compounds with an acceleration of anion diffusion at low temperature (Barr et al. 1960). In MgO, the diffusion of oxygen shows, at low temperature, an enhancement attributed to pipe diffusion with measurement of oxygen diffusion in a high-purity sample (Yang & Flynn 1994) correlated to dislocation densities (Van Orman & Crispin 2010, Landeiro Dos Reis et al. 2022).

Thus, pipe diffusion may influence the climb velocities, with a significant enhancement at low jog density. Full mathematical expressions for climb velocity accounting for the effect of pipe diffusion are given by Caillard & Martin (2003). The pipe diffusion then has the effect of balancing the jog formation energy in the activation energy of the climb process. The activation energy for climb becomes closer to U_{sd} (activation for pipe compensating the jog formation energy contribution). Another consequence of efficient pipe diffusion is the fact that climb velocity scales with respect to the climb force with an exponent greater than 1 and being potentially climb force intensity dependent.

4. THE CLIMBING DISLOCATION

4.1. Influence of Character

The simplest case corresponds to undissociated edge dislocations. In that case, the dislocation core can be approximated by the edge of an extra half-plane where point defects can be absorbed or emitted at jogs (**Figure 4*a***). This causes the jogs to move and the dislocation to climb. The climb of mixed dislocations possessing appreciable edge components proceeds by the same mechanism as for the pure edge dislocation. However, the absorption of vacancies at the jogs may be more complicated because glissile atomic rearrangements at the jogs are often necessary (Ballufi 1969). In case of (pure) screw dislocations, it is known experimentally (e.g., Amelinckx et al. 1957) (see **Figure 2*a***) that vacancies become absorbed in the core. By solving the equilibrium equation of a dislocation subjected to an external stress, an osmotic force, and a line tension, Weertman (1957) showed that the line spontaneously assumes the form of a helix (characterized by the pitch p and the diameter d) with the axis parallel to the Burgers vector (e.g., in gadolinium gallium garnets, Matthews et al. 1973; in calcite, Barber et al. 2007). The equilibrium ratio $R_c = 2\pi p/d$ has been calculated theoretically and was found to be $R_c = 1.4 \pm 0.5$ (Veyssière & Grilhé 1971). Recently, Liu et al. (2017) developed a 3D DD model coupling dislocation glide and climb to figure out the intrinsic formation mechanism of helical dislocations. They show that the number of turns increases linearly with the external stress and that the formation time of helical dislocations decreases exponentially with the vacancy concentration. Using electron tomography, Mussi et al. (2021a) have shown that, in MgO undergoing electron irradiation, the first stages of formation of helical dislocations show a morphology that deviates from the ideal cylindrical helix, revealing the existence of preferential mixed climb planes (**Figure 6**). Amelinckx et al. had already raised this hypothesis in 1957 in NaCl (see **Figure 2*b***).

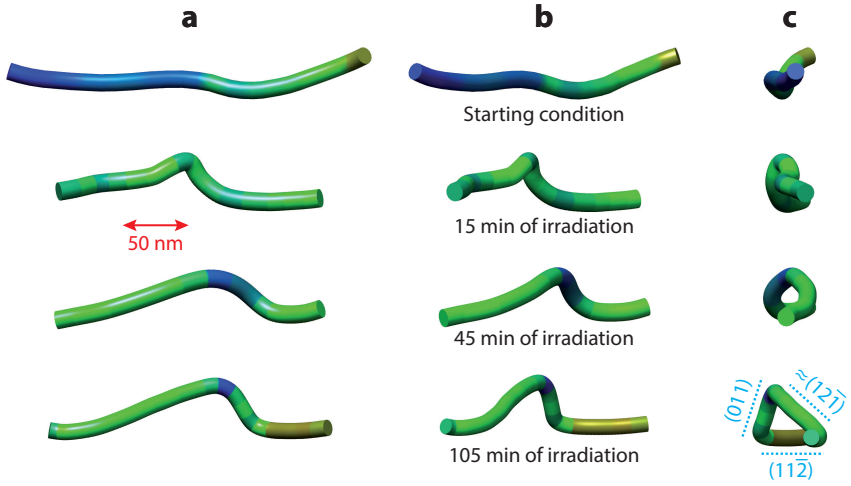

Figure 6

Helix formation in MgO during electron irradiation. Shown are tomographic reconstructions. The left column (*a*) shows the dislocation at 90° from the edge-on configuration. The central column (*b*) shows it at 45° from the edge-on configuration. The dislocation is seen approximately edge-on in the right column (*c*). Going from top to bottom corresponds to increasing irradiation times. Note in panel *c* that after 100 min, the helix is not circular anymore with the appearance of preferential mixed climb planes. Figure adapted with permission from Mussi et al. (2021a) (CC BY 4.0).

4.2. Climb of Dissociated Dislocations

In fcc crystals, jogs are dissociated as the dislocation cores are. Hirsch (1962) postulated the structures of jogs along dissociated dislocation in fcc metals. As guessed by Hirsch, atomistic calculations confirm that the stable configuration of the jog pair configuration corresponds to an obtuse and an acute jog lying in a (111) dense plane along the [112] direction (**Figure 4*b***). Jog segments are of edge character. For the acute jog, dislocation segments are thus of Lomer-Cottrell type, while for the obtuse jog, segments are of Hirth type. The geometrical stair rods segments, formed at the intersection of two dense planes, are then expected to increase the friction force of a dissociated dislocation carrying an extended double jog.

The mechanism at the origin of the nucleation of a jog pair along a dissociated dislocation is complicated. Stroh (1954) proposed that formation of a constriction before the aggregation of vacancies would be required for the nucleation of a double jog. However, different scenarios have also been proposed (Thomson & Balluffi 1962, Escaig 1963, Grilhé et al. 1977, Cherns et al. 1980, Argon & Moffatt 1981). For instance, Thomson & Balluffi (1962) consider the nucleation of prismatic vacancy loops at one of the Shockley partial dislocations that then propagates across the stacking fault toward the other partial. This mechanism has been observed by Cherns et al. (1980), and Grilhé et al. (1977) have computed the critical size of the prismatic loop. More recently, the activation pathway for extended double jog nucleation in fcc crystals has been studied using specific molecular dynamics simulation (Sarkar et al. 2012, Baker & Curtin 2016). Such calculations confirm that a small prismatic loop can form by aggregation of four vacancies and triggers the nucleation of the double jog as proposed by Thomson & Balluffi (1962). Argon & Moffatt (1981) propose rather that climb of the dislocations is controlled by vacancy emission from extended jogs. This climb mechanism governed by vacancy evaporation at the jogs along the dislocation line was proposed by Friedel (1964) when jog concentrations along dislocation lines are too low.

However, the probability of vacancy emission from a jog as computed in recent calculations is very low (Baker & Curtin 2016).

4.3. Climb Dissociation

The transition from an elementary solid to a compound induces complications, for example, at the level of dislocations. The presence of two or more sublattices and large Burgers vectors suggests more complex core structures than in metals with, as we shall see, major implications on plasticity. The presence of several different atomic species requires that the edge dislocations have at least two extra half-planes. Climb dissociation is possible by a conservative process involving diffusion from one extra half-plane to the other along the fault plane (Bretheau et al. 1979). This configuration evolves through the absorption of point defects to the lowest-energy configuration associated with the equilibrium distance between partial dislocations. Climb under stress of a dislocation of this type must necessarily take place by uncorrelated absorption of point defects on each of the partial dislocations, as local fluctuations in the dissociation distance are unacceptable (Bretheau et al. 1979). This phenomenon has been documented in spinel oxides (Veyssière et al. 1978), in Mg-Al spinel (Doukhan et al. 1982, Donlon et al. 1998), in faulted loops forming during dipole breakup (see Section 5.1) in sapphire (Phillips et al. 1982a, Tang et al. 2003), in Ni_3Al (Douin et al. 1988), in YBaCuO (Zheng et al. 1993), in superhydrous B (Mussi et al. 2013), and in dislocation networks in nickel ferrite (Veyssière et al. 1976) and Mg-Al spinel (Donlon et al. 1979).

If the partial dislocations are very far apart, they can move by glide in an uncorrelated way. The glide of the partial dislocations is then opposed by a dragging force due to the creation of additional surface of climb fault. This fault can follow the displacement of partials only by diffusion. We are then in the conditions of a viscous drag governed by diffusion (Bretheau et al. 1979).

If the partials separation distance is small, the climb fault inhibits the possibility of dislocations moving by glide. This can have considerable consequences on the plasticity as observed on $SrTiO_3$ at high temperature.

The plasticity of $SrTiO_3$ single crystals compressed along <100> shows three distinct regimes as a function of temperature (Brunner et al. 2001) (see **Figure 7**). Below ca. 1,000 K (regime A on **Figure 7**) plasticity is carried by thermally activated glide of <110>{110} dislocations (Brunner et al. 2001) well described by a kink-pair mechanism (Carrez et al. 2010). Then starts a second regime (B: 1,050–1,500 K) characterized by a very strong hardening leading to an essentially brittle behavior followed by a third regime (C: 1,500–1,800 K) where ductility is observed again with a flow stress rapidly decreasing when temperature is increased. The inverse ductile-brittle transition is due to a change in the core structure from a glide dissociation at low temperature (**Figure 8*a***) to a climb dissociation (**Figure 8*b***) that is more stable than dissociation on the slip plane (Hirel et al. 2016). Experimental evidence for this climb dissociation came from a high-resolution transmission electron microscopy (TEM) study (Zhang et al. 2002) on bicrystals diffusion bonded at 1,700 K (**Figure 8*c***). Sigle et al. (2006) have shown that regime C results from climb of <110> dislocations.

5. HOW DOES CLIMB CONTRIBUTE TO CREEP?

5.1. Climb as a Recovery Mechanism

Having established the fundamental mechanisms and relationships related to dislocation climb, we now turn to creep in an attempt to relate the behavior to microscopic mechanisms. Early on, Dorn (e.g., 1954) performed a rigorous analysis of creep data and derived constitutive equations that are still the basis of most rheological laws today. His conclusions are summarized by the following

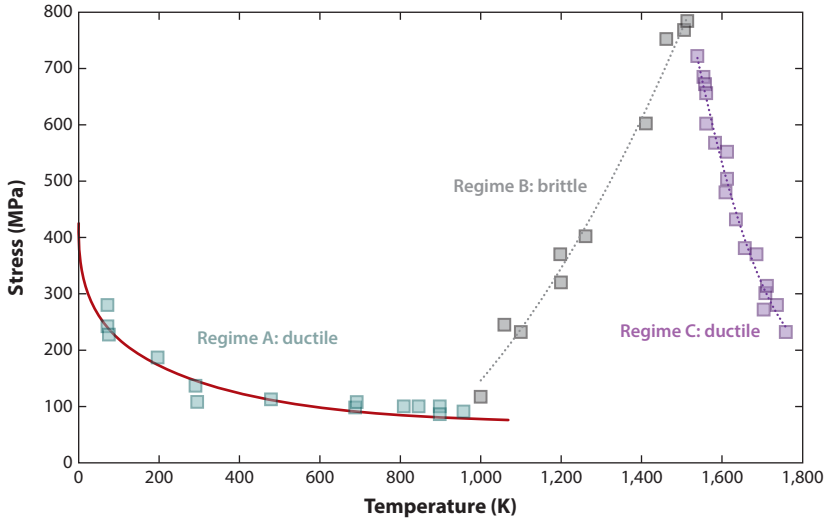

Figure 7

Compression of $SrTiO_3$ single crystals along ⟨001⟩. Symbols represent data from Gumbsch et al. (2001) describing the dependence of the critical flow stress on temperature. The low-temperature ductile regime (*green*) is well described by glide of ⟨110⟩{110} dislocations governed by the kink-pair mechanism. The red line is the model from Carrez et al. (2010). In the intermediate temperature interval (*gray*), there is no measurable plastic deformation. The symbols indicate fracture stress. The high-temperature regime (*purple*) is due to climb of <110> dislocations. Dotted lines in regimes B and C were added as visual guides only.

relationship giving the creep rate $\dot{\varepsilon}$:

$$\dot{\varepsilon} = A\sigma^n \exp\left(\frac{-Q}{kT}\right), \qquad 13.$$

where A and n are constants, k is the Boltzmann constant, T is the temperature, and Q is the activation energy. Let us note immediately that as long as A and n cannot be rigorously deduced from physical parameters of the material, we cannot consider that a reliable theoretical description is reached. This is a point that is particularly important to keep in mind in Earth sciences where these laws must be extrapolated over several orders of magnitude of strain rate. However, a

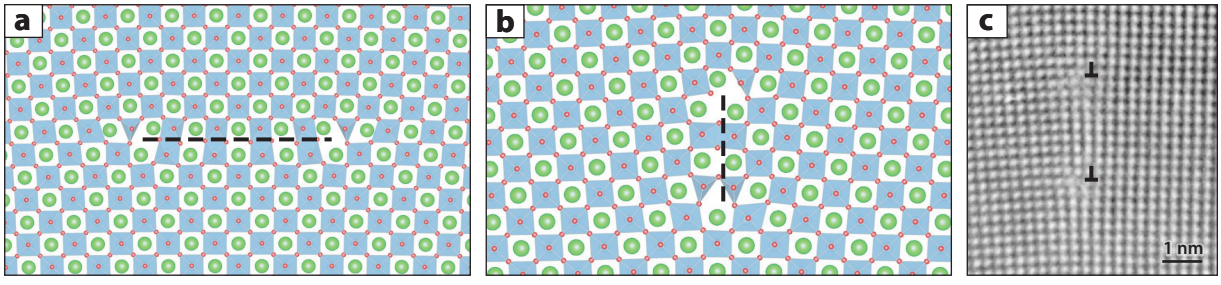

Figure 8

Core structures of [110] edge dislocations in $SrTiO_3$. (*a*) At low temperature the dislocation is dissociated in the $(1\bar{1}0)$ glide plane. Sr ions are displayed as large spheres, oxygen as small red spheres, and Ti ions are within transparent blue polyhedra. (*b*) At high temperature the dislocations are dissociated in the (110) climb plane. Panels *a* and *b* adapted from Hirel et al. (2016) (CC BY-NC-ND 4.0). (*c*) High-resolution transmission electron microscopy image of an [110] edge dislocations dissociated by climb. This image is taken from a bicrystal specimen containing a low-angle <110> tilt grain boundary. Panel *c* adapted with permission from Sigle et al. (2006).

fundamental contribution by Dorn is to have linked Q to the activation energy of self-diffusion. He thus established (in pure metals at that time, but it can be generalized) that self-diffusion is the ultimate rate-controlling process of the steady-state creep and immediately made the connection with climb of dislocations (an idea taken up in Mott 1951). Many creep models have been proposed in the literature. The common point of these approaches is to make the steady state emerge from the balance of two competing processes: hardening and recovery. The steady-state creep rate $\dot{\varepsilon}_s$ is then expressed by the Bailey-Orowan equation $\dot{\varepsilon}_s = r/h$, where r and h are the recovery and strain hardening rates, respectively. Although several mechanisms can be involved in recovery (e.g., cross-slip), we focus here on climb-controlled recovery mechanisms. The archetype of these models is the one proposed by Weertman (1955). He considers a very simplified situation in which sources produce dislocations that glide in parallel planes [a situation commonly encountered, for instance, in hexagonal or rhombohedral materials when basal slip is much easier, e.g., in sapphire (Pletka et al. 1982)]. The hardening results from the long-range elastic interaction between these dislocations and more precisely from the blocking of the edge segments that form dipoles. The recovery results from annihilation of these dipoles by climb allowing further glide. Theoretical calculations show that straight dipoles are unstable (Phillips et al. 1982b, Junqua & Grilhé 1984). Small amplitude fluctuations resulting from self-climb are energetically favorable for wavelengths much greater than the dipole width. This results from a balance between the dislocation self-energy and the elastic interaction energy. The dislocation dipole breaks up into a string of circular dislocation loops, the distance between the loops resulting from the dominant fluctuation wavelength. The coupling of DD with the diffusion theory of vacancies already described (Gao et al. 2011) has allowed modeling of the dipole breakup process showing that small fluctuation amplitudes and large fluctuation wavelengths are energetically favorable to the occurrence of breakup. Liu et al. (2020) show that loops are pinched off sequentially from the tip of the dipole rather than the dipole spontaneously breaking up into a string of loops, confirming the observations of Lagerlöf et al. (1989) and Tang et al. (2003) that nucleation of this process appears to be more favorable at the end of closed-ended dipoles. Indeed, electron microscopy has provided much evidence that validates these theoretical assumptions. The observations used to develop these models were mainly on sapphire (Phillips et al. 1982b, Pletka et al. 1982, Tang et al. 2003), but examples can be found in other materials—for example, observations have been reported since Braillon et al. (1978). **Figure 9** presents similar evidence in olivine single crystals deformed at temperatures lower than 1,000°C (see description of these experiments in Demouchy et al. 2013). Although at these temperatures and in single crystals, very few slip systems are active (only [001] slip is active), we observe the presence of entanglements. Within these entanglements, one can recognize the presence of dipoles. Some of them show pinches or even alignments of small loops that represent a more advanced stage. In laboratory experiments, this diffusion-limited mechanism does not allow a sufficiently efficient recovery and a steady state cannot be reached, leading to a limited ductility. However, a higher ductility can be expected if the strain rate is low enough to allow time for this mechanism to counteract the hardening.

The 2D models of dislocation dynamics coupled with the diffusion of vacancies allow us to further develop the approach outlined in the Bailey-Orowan equation and to provide a basis for modeling Weertman creep (Keralavarma et al. 2012, Boioli et al. 2015a). Hardening is described through the evolution of the microstructure and the multiplication of dislocations by sources. The recovery can be taken into account by the annihilation of dipoles as described above. Although very simplified in terms of description of the microstructure, these models already reproduce the main characteristics of high-temperature creep, i.e., a stress exponent and an activation enthalpy in agreement with experimental data (Keralavarma et al. 2012, Boioli et al. 2015a). They also allow verification of the commonly accepted hypotheses on the Weertman creep. Indeed, if climb is not

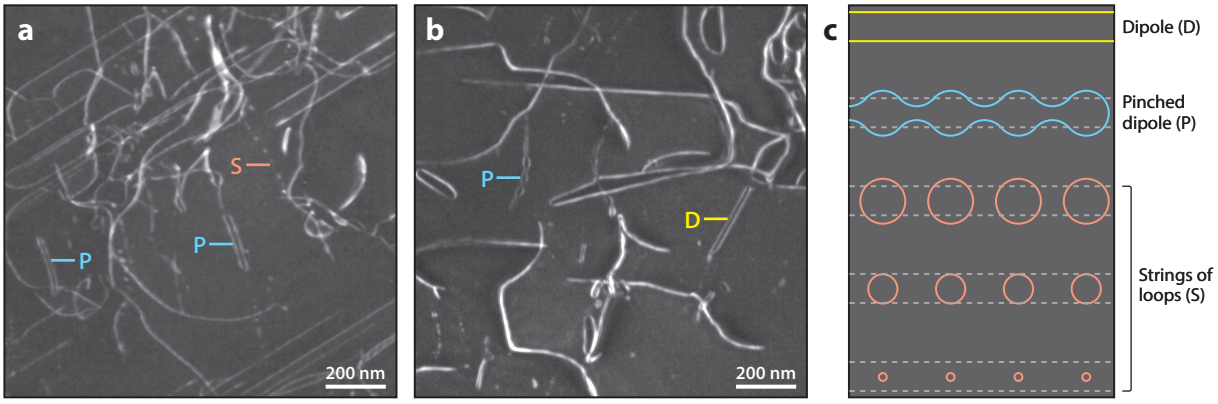

Figure 9

Evidence of recovery by dipole breakup in experimentally deformed olivine. (*a*) Specimen deformed at 850°C, 7.06×10^{-6}/s. (*b*) Specimen deformed at 900°C, 1.01×10^{-5}/s. Panels *a* and *b* adapted with permission from POEM 11 of Demouchy et al. (2013) (CC BY-NC-ND 4.0). (*c*) Under the action of pipe diffusion, instabilities develop on the dislocation lines of the dipole, which pinch and break up into sessile loops. The loops are sinks for point defects and progressively shrink and disappear as a result of bulk diffusion. Panel *c* adapted from Boioli et al. (2015b).

allowed, the strain quickly saturates in creep (i.e., under constant load) by dislocations locking (the dipoles previously described). The activation of climb that allows the annihilation of these dipoles allows the establishment of a steady state. However, it can be seen that climb, which controls the strain rate, contributes only marginally to the total plastic strain (**Figure 10**).

The mechanism of dipole annihilation is not specific to all materials and requires a thorough investigation in TEM. In general, the demonstration of the activation of climb is not easy. Generally speaking, the most used microstructural criterion is the formation of subgrain boundaries and polygonization. Here, recovery driven by the reduction of the energy of the dislocation network does not result from the annihilation of dislocation pairs but by the transport (and further incorporation) of dislocations from subgrain interiors to subgrain boundaries. In this dynamic context, the preservation of well-organized subgrain boundaries [i.e., consisting of parallel and equidistant dislocation lines (see **Figure 11**)] requires climb (Mott 1953, Friedel 1964). Further evidence of climb activation in the formation of subgrain boundaries is the frequent observation of climb dissociation in these networks as already reported above in nickel ferrite (Veyssière et al. 1976) and Mg-Al spinel (Donlon et al. 1979). Although the role of climb in the formation of subgrain boundaries and polygonization has been considered for a long time, its complex modeling is still in its infancy. Gu et al. (2016) rely on Green's function formulation to study the stability of low-angle grain boundaries by climb of the constituent dislocations. They show that a perturbed low-angle tilt boundary relaxes back to its equilibrium distribution on a timescale that is proportional to the square of the perturbation length scale and inversely proportional to the point defect diffusivity. This climb-based recovery occurs predominantly through pipe diffusion at low temperatures and bulk diffusion at high temperatures (Gu et al. 2018).

Polygonization with formation of subgrain boundaries was reported as early as 1960 by Amelinckx & Strumane (1960) in sodium chloride. In this study, polygonization kinetics was exploited to obtain the energy of jog formation. In a similar approach, Goetze & Kohlstedt (1973) performed annealing on naturally deformed peridotites to quantify the degree of recovery by counting the number of dislocations that have climbed in subgrain boundaries. In minerals, the presence of well-organized subgrain boundaries has thus been the main marker of the activation of dislocation climb in both the analysis of laboratory deformation microstructures (e.g., quartz,

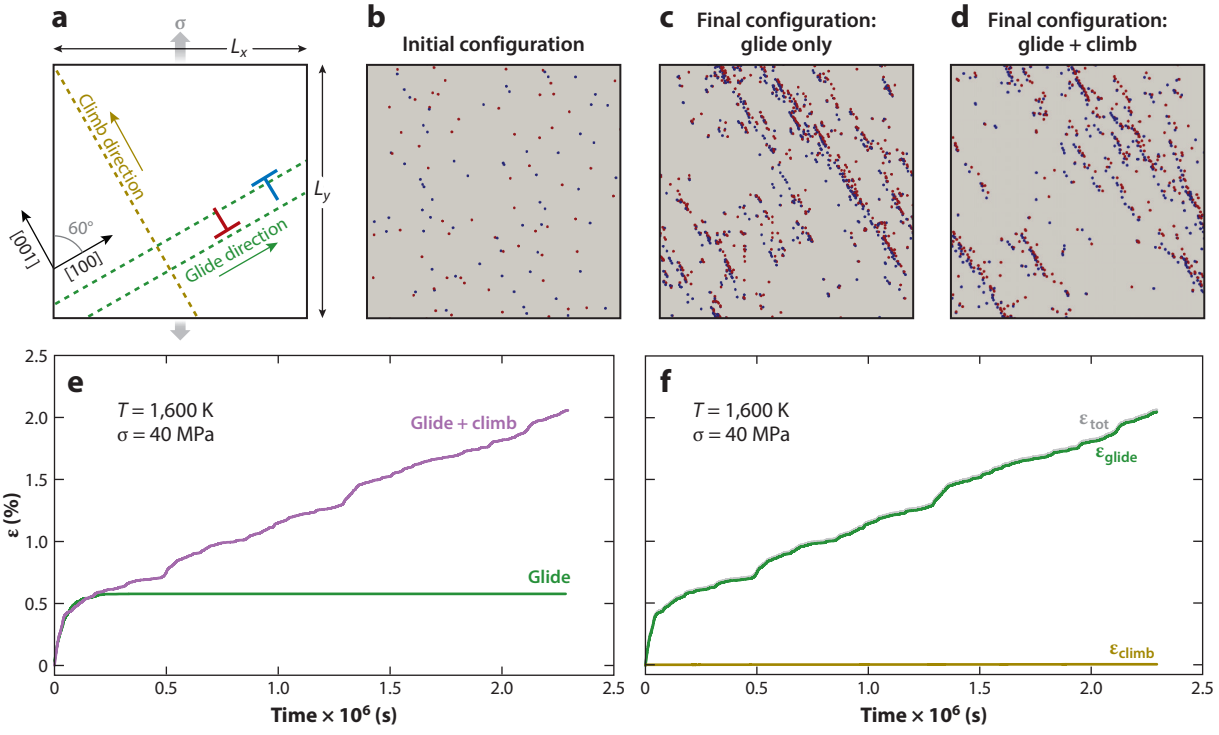

Figure 10

Two-dimensional dislocation dynamics creep modeling in olivine. (*a*) Sketch of the 2D simulation box showing the geometry of the single slip conditions used. The angle between the loading axis and glide displacement direction is 60°. (*b*) Initial dislocation microstructure. (*c*) Final dislocation microstructure obtained with glide only activated. (*d*) Final dislocation microstructure obtained with glide and climb activated simultaneously. (*e*) Plastic deformation ε versus time produced with glide only (*green*) and glide plus climb (*purple*). (*f*) The plastic strain produced by glide (*green*) and climb (*gold*) compared with the total plastic strain (*gray*). Total plastic strain and strain produced by glide are almost indistinguishable. Figure adapted with permission from Boioli et al. (2015a) (CC BY 3.0).

Cordier & Doukhan 1989, Tullis & Yund 1989) and the attempt to decipher the microstructures of natural samples (e.g., hornblende, Skrotzki 1992; garnet, Hawemann et al. 2019; quartz, White 1977; olivine, Green 1976, Kirby & Wegner 1978).

On a more mesoscopic scale, in many materials, recovery results in patterning, which often takes the form of cells containing fewer dislocations separated by more or less organized dislocation walls. The two mechanisms described above (annihilation of pairs of dislocations and formation of subgrain boundaries) are therefore two components of patterning. The description of this phenomenon at this scale is a complex one because it requires describing the collective behavior of a large number of dislocations. Let us specify at once that several local interaction mechanisms can contribute to patterning—for example, cross-slip, which is not discussed here, our goal being to clarify the role of climb. DD modeling is nowadays the best tool to address this question, which is one of the most disputed challenges. Simple simulations of parallel dynamics of edge dislocations in a 2D hexagonal lattice performed by Bakó et al. (2006) already showed that activation of climb is necessary for cell structures to emerge. A more sophisticated model was proposed recently by Kohnert & Capolungo (2022). Their 3D DD model, applied to pure iron, is able to describe the climb of generalized dislocation geometries (including mixed character segments and junctions) through bulk vacancy transport in a manner that accounts for heterogeneity in the

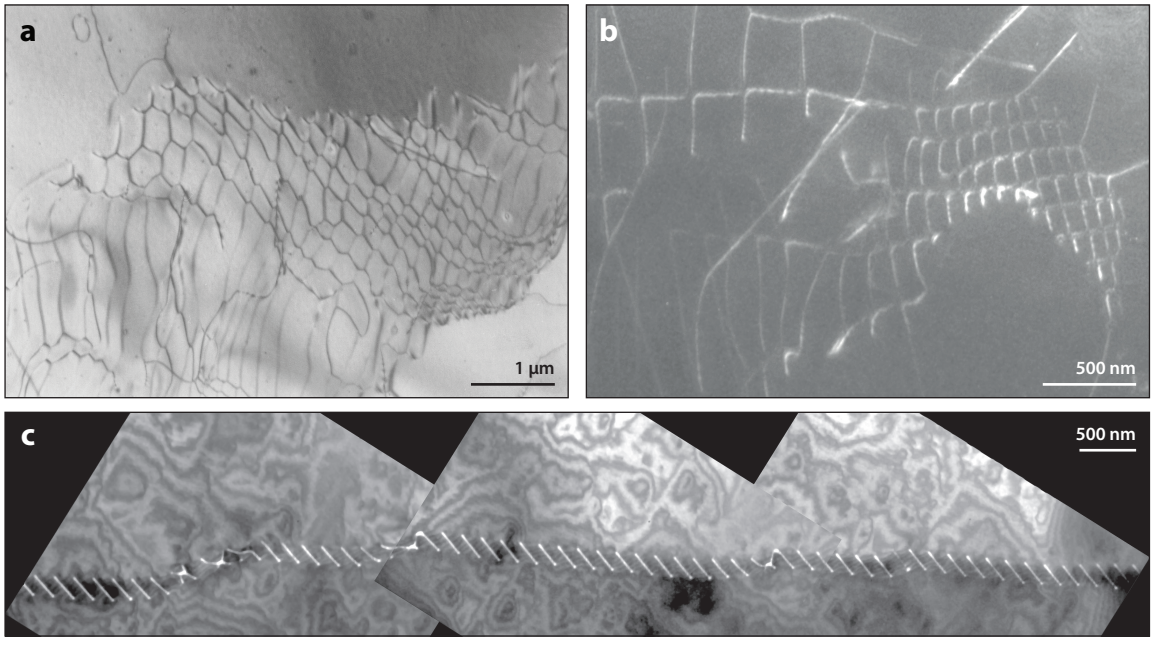

Figure 11

(*a*) Synthetic quartz experimentally deformed at 700°C, 800 MPa; transmission electron microscopy (TEM) bright-field $g : 01\bar{1}1$. Panel adapted with permission from Cordier & Doukhan (1989). (*b*) Superhydrous B sample experimentally deformed at 20 GPa and 1,000–1,100°C; TEM weak-beam dark-field $g : 303$. Vertical dislocations are of the [001] type; horizontal dislocations are of the [101] type. Panel adapted with permission from Mussi et al. (2013). (*c*) Garnet from a quartzofeldspathic rock within a shear zone of South Madagascar; TEM weak-beam dark-field. Panel adapted with permission from Martelat et al. (2012).

dislocation arrangement. This model reproduces quantitatively the logarithmic trend of recovery observed experimentally demonstrating that climb is the controlling mechanism for static recovery in pure metals. They also show that microstructures with geometrically necessary dislocations show significantly slower recovery than the other networks.

5.2. Climb as a Deformation Mechanism

In the recovery-controlled creep model, climb is not expected to contribute significantly to the total strain (**Figure 10**). Yet this assumption has often been questioned. Analyzing the shape change of olivine single crystals deformed along $[101]_c$ at 1,600°C, Durham & Goetze (1977) proposed that climb contributed 10–20% to the strain rate. At about the same time, White (1977), but also Ball & White (1978) and Ball & Glover (1979), raised the question of an effective contribution of climb in the plastic deformation of quartz by attempting to evaluate its contribution to the plastic deformation rate. However, as the author acknowledges, "The greatest source of inaccuracy [. . .] is the lack of precise diffusion data" (White 1977, p. 155). This approach was taken up in materials science in the 1990s in $MoSi_2$ (Evans et al. 1997) and titanium-aluminum intermetallics and alloys (Kad & Fraser 1994, Lin et al. 1999). In particular, the role of climb in promoting ductility and influencing the ductile-brittle transition was highlighted (Evans et al. 1997, Lin et al. 1999).

5.2.1. Mixed climb. From a fundamental point of view, to assess the respective contributions of glide and climb, we need to be able to compare the glide and climb velocities (as well as the respective proportions of the different dislocations). In practice, these velocities are difficult to measure,

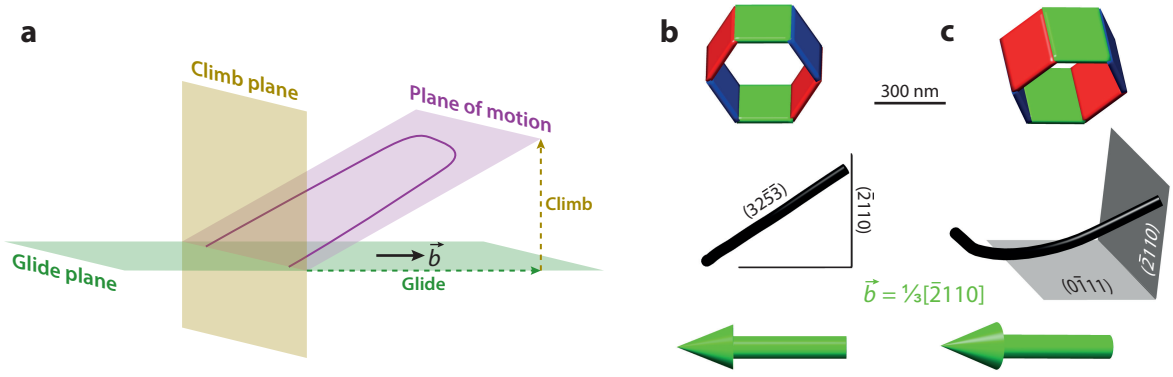

Figure 12

(*a*) Sketch of a dislocation loop moving by combined glide and climb in a plane whose orientation is intermediate between the glide plane (containing the Burgers vector $\vec{b}$) and the climb plane, which is perpendicular to it. (*b*) Quartz from a granulite: tomographic reconstruction of a 1/3[$\bar{2}$110] dislocation (the *green arrow* represents the Burgers vector) moving in a plane that is neither the glide plane (0$\bar{1}$11) nor the climb plane ($\bar{2}$110). (*c*) Same dislocation as in panel *b* viewed from the side. See **Supplemental Movie 1**, which corresponds to panels *b* and *c*.

Supplemental Material >

but a recent study based on in situ deformation experiments in the TEM on TiAl metallic alloys revealed displacement velocities of the same order of magnitude at 790°C for both mechanisms (Galy et al. 2023). In this case, dislocations moving simultaneously by glide and climb move in undefined planes whose orientation is intermediate between the glide plane and the pure climb plane (**Figure 12**). This is now known as mixed climb. Such configurations had already been highlighted by Malaplate et al. (2004), Couret (2010), and Voisin et al. (2016) in these TiAl alloys and provide valuable microstructural evidence of climb's real contribution to deformation. In these alloys, the aforementioned authors point out that the mixed climb deviation increases dislocation mobility because ordinary 1/2<110] dislocations are subject to strong lattice frictions on screw segments in their {111} glide planes due to their core structure. From the microstructural point of view, evidencing dislocation climb requires precise characterizations of dislocation microstructures to demonstrate that dislocation lines do not belong to their glide planes. Because TEM provides 2D projections, tilting experiments are necessary to make these characterizations (see Malaplate et al. 2004, Couret 2010, Voisin et al. 2016). Recently, this has been made more widely available by the development of electron tomography of dislocations (Feng et al. 2020). The difficulty of this technique is to keep the diffraction contrast of dislocations rigorously constant over a large range of tilt orientations. **Figure 12** shows an illustration of such characterization in naturally deformed quartz.

5.2.2. Pure climb. In 1964, Friedel proposed a deformation mechanism that generalizes diffusion creep formalized by Nabarro and Herring where the displacement by climb of dislocations being sources and sinks of vacancies would be the strain-producing mechanism (**Figure 13*a***). Nabarro (1967b) proposed a treatment of this problem where the steady state emerges from the balance between the hardening resulting from the multiplication of dislocations (increase of internal stress) and the recovery (decreasing internal stress) due to the dislocation climb. Dislocation multiplication results from the operation of Bardeen-Herring sources.

The steady-state strain rate resulting from this mechanism is given (Nabarro 1967b) by the equation

$$\dot{\varepsilon}_N = \frac{Db\sigma^3}{\pi kT\mu^2} / \ln\left(\frac{4\mu}{\pi\sigma}\right). \qquad 14.$$

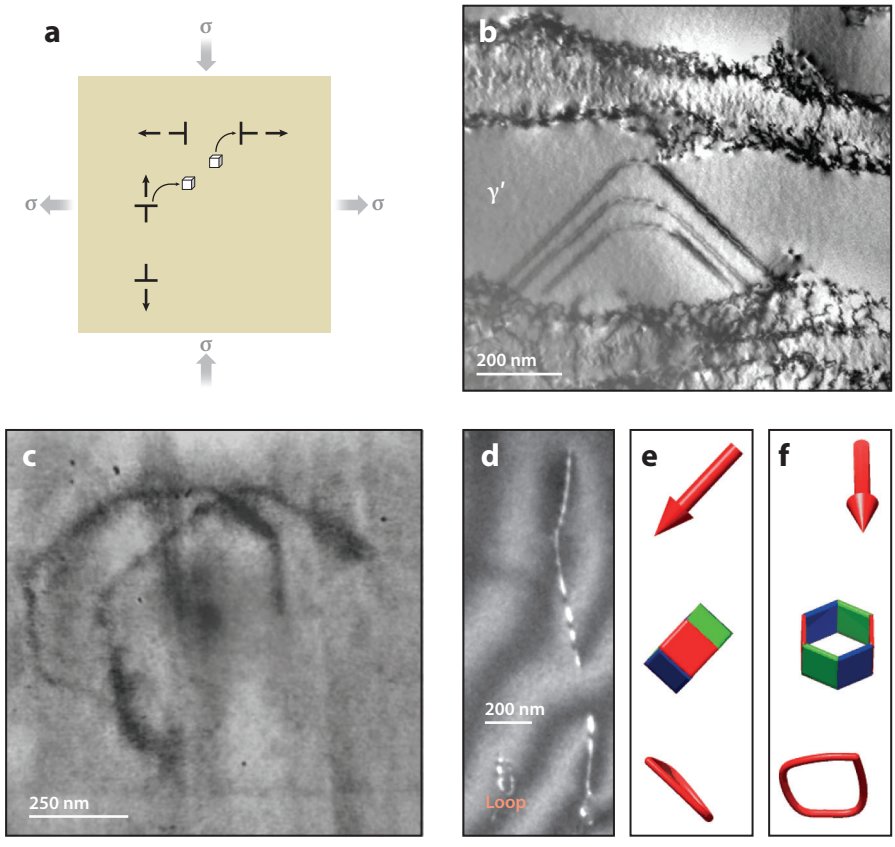

Figure 13

(*a*) Plastic deformation by pure climb with two dislocation families exchanging vacancies. (*b*) Nickel-based superalloy CMSX-4; [010] edge dislocation penetrating the γ′ phase by climb. Panel adapted with permission from Epishin & Link (2004). (*c*) Icosahedral Al–Pd–Mn quasicrystals. Two loops expanding by climb in a twofold plane are observed in situ at 720°C. Panel adapted with permission from Mompiou et al. (2004). (*d*) Quartz from the Main Central Thrust of Northwest India. The loop has a $1/3[11\bar{2}0]$ Burgers vector (*red arrow* in panels *e* and *f*), weak-beam dark-field $g: 0\bar{1}11$. (*e*) Same loop as in panel *d*; tomographic reconstruction showing the loop edge-on. Being normal to the Burgers vector, it is a pure climb configuration. (*f*) Same loop as in panel *d* seen from the front. See **Supplemental Movie 2**, which corresponds to panels *d–f*.

Mompiou & Caillard (2008a) argued, however, that the stress dependence of pure climb creep can be larger than 3, in particular when the nucleation of jog pairs and their interaction with solute atoms need to be taken into account.

Supplemental Material >

In metals, glide is usually easier than climb. The demonstration of this pure climb mechanism can be done only if glide is inhibited. This is geometrically possible in crystals with hexagonal symmetry if the compression axis is parallel to the [0001] axis (in the absence of pyramidal slip). Based on this approach, the mechanism of pure climb has been experimentally demonstrated on single crystals of magnesium (at 340–630°C, i.e., 0.66–0.98 T/T_m) by Edelin & Poirier (1973a,b), of beryllium (at 350–1,000°C, i.e., 0.4–0.8 T/T_m) by Le Hazif et al. (1973), and of sapphire (at 1,600–1,800°C, i.e., 0.8–0.9 T/T_m) by Firestone & Heuer (1976). Note that in the case of sapphire single crystals deformed along [0001], Groves & Kelly (1969) had already proposed deformation by a

pure dislocation climb mechanism based on analysis of the geometry of the deformed specimens. In minerals similar experiments (compression of single crystals along the *c* axis) were performed by Ball & Glover (1979) on single crystals of synthetic quartz (OH content in the range 50 to 160 ppm). The deformation conditions were 300 MPa, 500°C–10^{-6}/s, and 700°C–10^{-7}/s. Compared to the previous cases, these conditions correspond to lower temperatures (0.4–0.5 T/T_m), the climb being activated by the diffusion of OH groups (Cordier & Doukhan 1989).

A striking illustration of the role that climb can play in the deformation of solids is provided by the study of quasicrystals. Icosahedral quasicrystals are very brittle at low temperatures but exhibit very high ductility at high temperatures (above ca. 0.7 T_m), which is essentially due to the movement of dislocations. However, in the quasicrystalline structure, the dense planes are very corrugated, which makes shearing them very difficult (Caillard et al. 2002, Mompiou & Caillard 2014). The brittleness at low temperatures is then related to the impossibility of dislocation glide. TEM investigations of Al-Pd-Mn quasicrystals deformed in situ and ex situ at high temperature have demonstrated that dislocations can move (Wollgarten et al. 1995; Caillard et al. 2000, 2002; Mompiou et al. 2003; Mompiou & Caillard 2008b) by climb only. In fact, Gratias et al. (2006) have demonstrated that edge dislocations moving by pure climb are the only dislocation motion that keeps the internal tiling coherent. A plasticity model based on Nabarro (1967b) has been proposed by Mompiou & Caillard (2008b) for Al-Pd-Mn that fully reproduces the characteristics observed experimentally, including a high strain hardening at yield, a steady-state flow stress two times higher than the elastic limit, and two-stage relaxation curves.

In the γ phase of TiAl, several pieces of evidence of pure climb of dislocations have been documented. In situ heating experiments at 750°C confirmed that ordinary 1/2<110] dislocations are able to move viscously in {110} planes by pure climb of straight edge segments parallel to the <112> directions (Malaplate et al. 2004), and stereomicroscopic observations of specimens crept at 850°C under 150 MPa have revealed evidence of pure climb of [001] dislocations in (001) (Naanani et al. 2018).

This pure climb creep mechanism has also been documented in the high-temperature creep of Y_2O_3 (Gaboriaud 1981). In this oxide, dislocation glide is inhibited at high temperature by climb dissociation of <100> dislocations. Here we find the same mechanism as that described in Section 4.3, which leads $SrTiO_3$ to deform by pure dislocation climb at high temperature (Sigle et al. 2006).

6. THE ROLE OF CLIMB IN THE RHEOLOGY OF PLANETARY MATERIALS

In minerals, numerous studies have invoked activation of climb, based on observations of varying degrees of substantiation. As we shall see, quantifying the contribution of this mechanism, particularly in natural deformations, is far from certain.

In calcite marble deformed within a greenschist facies, activation of climb-accommodated dislocation creep was inferred from the presence of low-angle boundaries suggesting recovery (Bestmann & Prior 2003). Experimentally, Braillon et al. (1978) have reported a creep behavior with a power law ($n \sim 3.5$) from single crystals deformed in compression along [111] for $T > 600$ K. TEM investigation showed recovery involving dislocation dipole breakup. Climbing dislocations were also reported associated with (0001)-slip in dolomite deformed at temperatures of 600–800°C (Barber et al. 1981).

The case of quartz has been better documented, although hydrolytic weakening makes the study of plasticity in this mineral more difficult to decipher. We have seen that very specific experiments (deformation of single crystals along the *c* axis) have shown that pure climb creep is possible in this mineral (Ball & Glover 1979). More generally, it has been shown that deformation of wet

synthetic crystals activates dislocation climb in conjunction with water precipitation in microbubbles and their subsequent ripening (Cordier & Doukhan 1989, McLaren et al. 1989). However, the ubiquity of the CPOs observed in quartz deformed in nature (e.g., Morales et al. 2011), and their importance to infer deformation temperatures, magnitude, and symmetry of strain and the deformation mechanisms, has led to focus on glide, although there is usually evidence of climb in the microstructures (Morales et al. 2011). An electron tomography study of naturally deformed quartz grains in a Bohemian granulite has enabled us to determine the components of the plastic deformation tensor from the dislocations observed by TEM (Mussi et al. 2021b). In particular, the components resulting from glide and climb are distinguished. This study showed that in this sample, the von Mises-Taylor criterion is satisfied thanks to the climb of $\langle c + a \rangle$ dislocations. In fact, verification of the von Mises-Taylor criterion is a problem that arises in quartz as in many minerals with low symmetries. Ball & White (1978) dealt with this issue, proposing that the solution lies in climb, with another solution being the activation of $\langle c + a \rangle$ glide. Our results show a mixed solution but one in which climb plays an important role. Recently, we have undertaken a detailed study of deformation microstructures in quartz from mylonites from Moine and Main Central Thrusts. In these specimens we find abundant evidence for mixed climb, with strong deviations between the plane of motion of dislocations and the glide plane demonstrating a climb velocity of dislocations very comparable to their glide velocity. To understand the significance of this result, it should be remembered that it concerns samples deformed under natural conditions, in particular with very low strain rates of the order of 10^{-13}/s. Thus, it is understandable that this gives the diffusion mechanisms more time to operate.

In feldspars deformed in the laboratory, clear evidence of dislocation climb with subgrain formation is found only at temperatures greater than 900°C (Willaime et al. 1979, Tullis & Yund 1992). In nature, feldspars deformed at greenschist (Hentschel et al. 2019) and lower amphibolite (White 1975) facies conditions show little or no evidence for climb. It seems that low Si/Al diffusivity makes dislocation climb inhibited unless the highest grades of metamorphism are reached.

The case of olivine has already been mentioned several times. In experiments, dislocation climb is attested as early as 1,000°C (Phakey et al. 1972). Durham & Goetze (1977) even proposed the use of Nabarro's (1967b) pure climb model to model the deformation of single crystals of olivine at 1,600°C along $[101]_c$. However, it is generally accepted that above 1,000°C, olivine deforms by recovery-controlled creep, with a behavior described by a power law (Goetze 1978). At the microstructural level, detailed analysis shows evidence of climb as from 850–900°C in the experiments: dipole breakup (**Figure 9**), helical dislocations, and pure climb loops (**Figure 14**; see also **Supplemental Movie 3**). As with quartz, the widespread observation of the development of CPO in natural samples testifies to the importance of dislocation glide (Ben Ismaïl & Mainprice 1998). CPOs are widely used to deduce flow in the upper mantle from seismic anisotropy. However, microstructural characterizations early on revealed the activation of climb (Green & Radcliffe 1972, Green 1976) and confirmed the use of the rheological laws used to describe recovery-controlled creep (see Section 5.1). Electron tomography analysis of the deformation microstructures of a mylonitic peridotite sample showed the presence of mixed climb (Demouchy et al. 2024). This observation needs to be confirmed, but it already raises the question of the role of climb in the upper mantle. Indeed, with depth, pressure tends to increase lattice friction on dislocations and thus decrease the efficiency of glide. This important question is addressed in greater detail below. However, it should be remembered that there are virtually no microstructural observations on mantle olivine samples from depths of over 200 km.

Supplemental Material >

Despite its importance in the rheology of the crust and mantle (up to the transition zone), garnet deformation is still poorly understood. The salient fact that emerges is that whenever

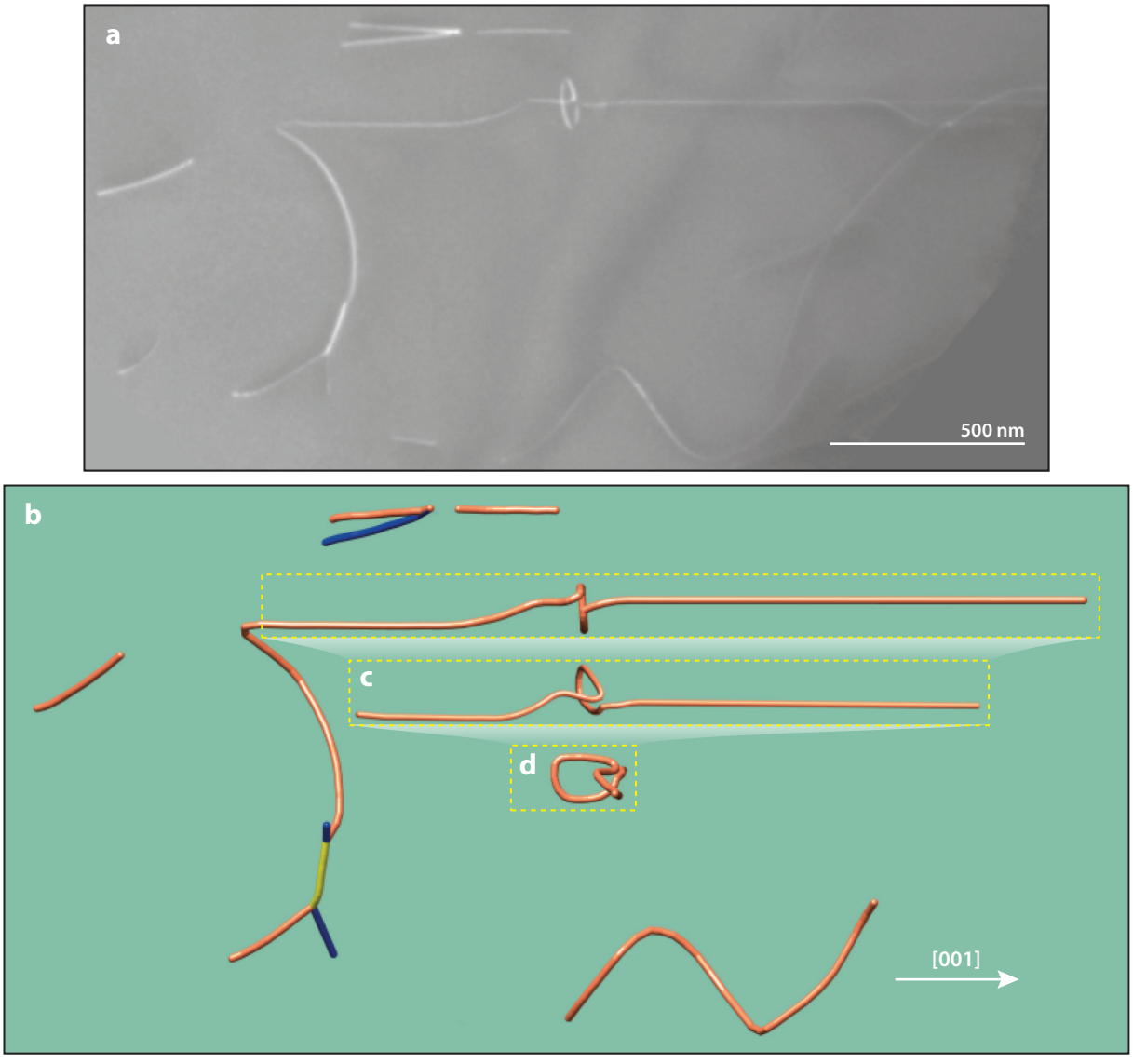

Figure 14

Olivine experimentally deformed at 900°C, 300 MPa. (*a*) Weak-beam dark-field $g : 2\bar{2}2$. The view is tilted by 22° around the vertical axis with respect to panel *b*. (*b*) Tomographic reconstruction. Here the Burgers vector [001] of coral-colored dislocations is horizontal. Blue dislocations are [100]. The yellow dislocation is a [101] junction. On top, a long [001] screw dislocation is interacting with a pure climb loop seen edge-on on this figure. At the bottom is a helix dislocation with [001] axis. (*c*) Same area as dotted box in panel *b* tilted at 45°. (*d*) Same area as dotted box in panel *b* tilted at 90°. See **Supplemental Movie 3**, which corresponds to this figure. Figure adapted with permission from Demouchy et al. (2014).

Supplemental Material >

the microstructures of samples showing macroscopic deformation indices have been analyzed, evidence of recovery (mainly subgrain boundaries) has been found (e.g., Ji & Martignole 1994, Prior et al. 2000, Hwang et al. 2003, Muramoto et al. 2011, Martelat et al. 2012, Hawemann et al. 2019). It seems that the ductility threshold of garnets is conditioned by the activation of diffusion (Voegelé et al. 1998). However, the respective efficiencies of glide and climb have not

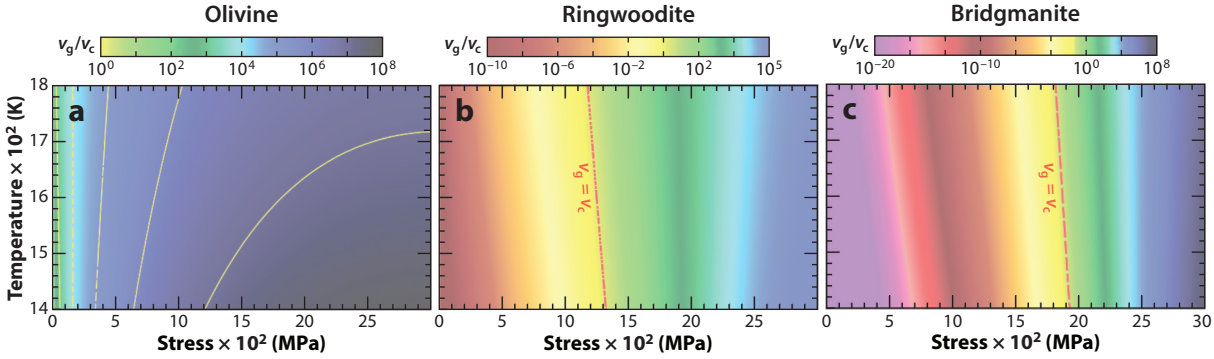

Figure 15

v_g/v_c is the ratio between the glide velocity and the climb velocity of dislocations. It is mapped here as a function of temperature and resolved stress for (*a*) olivine at ambient pressure, (*b*) ringwoodite at 20 GPa, and (*c*) bridgmanite at 30 GPa. The red line where $v_g = v_c$ indicates the transition between two regimes. At high stress (*green* to *blue*), glide is the strain-producing mechanism. At low stress (*yellow* to *purple*), climb dominates. Figure adapted with permission from Boioli et al. (2017) (CC BY-NC 4.0).

been determined in naturally deformed samples, partly due to the low density of free dislocations observed.

Studying the high-pressure phases of the mantle is more difficult, particularly as we have no access to samples that can tell us anything about the rheology of the deep mantle. The first parameter to consider here is pressure. At values corresponding to Earth's mantle (between 25 and 135 GPa for the lower mantle), pressure strongly affects bonds, resulting in an increase in elastic constants. But pressure also affects the structures of dislocation cores and therefore their mobility (Carrez & Cordier 2017). The general trend is toward phase hardening, which is well observed in experiments. Multiscale numerical modeling has recently made it possible to tackle these problems, starting from the atomic scale and taking into account the nature of bonds under pressure in order to build dislocation core models. The most successful example concerns wadsleyite (Castelnau et al. 2020) where atomic and polycrystal scales were bridged with excellent agreement with experimental data that show high stress levels. The second key parameter to consider is the strain rate, which should lead to lower stress levels at lower strain rates. Modeling thermal activation of dislocation glide makes it possible to model the influence of strain rate without extrapolation. However, it shows that the stress levels required to cause dislocations to glide are too high, compared with the stresses expected in the mantle (Ritterbex et al. 2015, 2016). One way of understanding the situation and its implications is to calculate the ratio between the glide velocity of dislocations and their climb velocity. This is shown in **Figure 15**. At high strain rates, at stresses of the order of gigapascals, deformation is possible by dislocation glide, as observed experimentally. At mantle stresses (1–10 MPa), however, only climb is possible. This situation is comparable to that of quasicrystals, except that the inhibition of glide is not due to plane corrugation but to pressure-induced hardening. Ritterbex et al. (2020) therefore sought to evaluate the efficiency of creep by pure dislocation climb based on the model of Nabarro (1967b). They show that this model leads to a viscosity of the order of 10^{21} Pa·s based on data for wadsleyite and ringwoodite, as well as that estimated for majorite. In the absence of the possibility of dislocation glide, the only alternative mechanism is diffusion creep, which can prevail over pure climb creep only for gain sizes of less than 0.1–1 mm.

The situation regarding glide is even more critical for bridgmanite due to the pressure range at which it is stable in the mantle, but also due to its crystallographic structure. **Figure 16*a*** shows the magnitude of the increase in lattice friction opposing glide in the lower mantle pressure range.

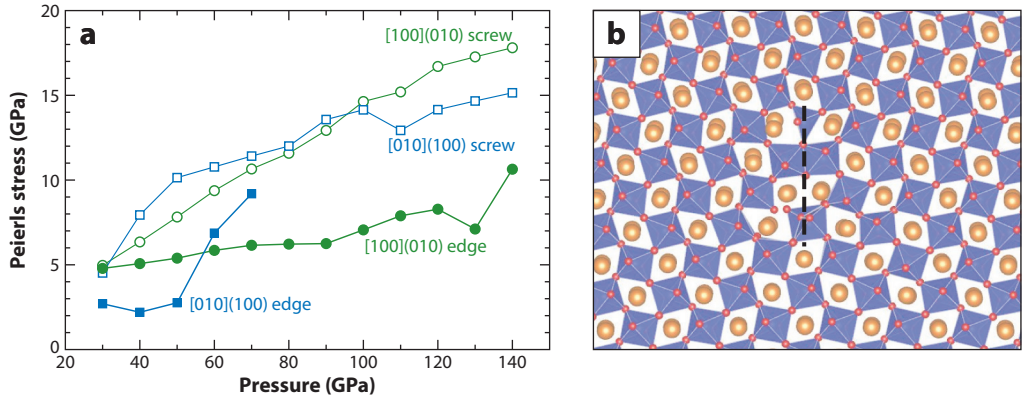

Figure 16

Bridgmanite $MgSiO_3$. (*a*) Evolution of lattice friction (Peierls stress) as a function of pressure. Panel adapted with permission from Hirel et al. (2014) (CC BY-NC 3.0)). (*b*) Core structure of the [001](100) edge dislocation at 30 GPa showing dissociation in the (001) climb plane. Panel adapted with permission from Hirel et al. (2016) (CC BY-NC-ND 4.0).

However, **Figure 15** already showed that at 30 GPa, i.e., in the uppermost lower mantle, very high stresses of several gigapascals are required to cause dislocations to glide (with a modest effect of temperature compared with that of pressure). In bridgmanite, which exhibits a perovskite structure, there is another phenomenon affecting edge dislocations that we have already encountered with $SrTiO_3$: climb dissociation. Atomic-scale calculations by Hirel et al. (2016) have shown that this mechanism is even more favorable in $MgSiO_3$ than in $SrTiO_3$. The distortion and tilts of octahedra in $MgSiO_3$ (which increase with pressure) increase the glide stacking fault energy and thus lower the energy barrier toward climb dissociation. **Figure 7** demonstrates the very strong implication of this core structure change (**Figure 8**) on the mechanical properties. We can therefore conclude from these calculations that dislocation glide is impossible in bridgmanite in the mantle. The climb dissociation configuration therefore favors their displacement by climb. Boioli et al. (2017) and Reali et al. (2019) have shown that pure climb (Nabarro) creep can account for the viscosity of the lower mantle. Note here that the same type of behavior is expected in $CaSiO_3$ davemaoite, a silicate also exhibiting a perovskite structure. In the end, in the lower mantle, only ferropericlase retains standard creep behavior, controlled by recovery [although slowed by slow diffusion under pressure (see Cordier et al. 2023)]. The view that emerges from this rapid overview is that for the silicates considered, from the transition zone downward, dislocation climb represents the dominant mode of deformation at work in mantle convection.

7. CONCLUDING REMARKS AND PERSPECTIVES

The climb mechanism has known various successes in mineral physics. Very early on, this mechanism, associated with high-temperature deformation, was considered to play a role in terrestrial deformation (Raleigh & Kirby 1970, Weertman 1970, Kirby & Raleigh 1973, Minster & Anderson 1980). The mechanisms considered were the climb-accommodated creep proposed by Weertman (1955), or the pure climb proposed by Nabarro (1967b). Indeed, as soon as it was released, the pure climb (Nabarro) creep mechanism was applied to various cases: e.g., sapphire (Groves & Kelly 1969, Firestone & Heuer 1976) or Mg single crystal–oriented along [0001] (Edelin & Poirier 1973a,b). In the latter case, Caillard & Martin (2003) suggested that a quantitative agreement of the experimental results with the pure climb creep model of Nabarro can be achieved once one takes account of the jog-pair nucleation. It should be noted that this option is not necessarily

retained today [despite that it has also been used to model creep of [0001] oriented alumina (Yi et al. 2006)], but it had the merit of showing that, given the uncertainties on the diffusion coefficients, dislocation climb was likely to contribute to the plastic strain. Little by little, however, this mechanism has been considered less and less, and, with a few rare exceptions, in mineral physics, the climb is considered only as a recovery mechanism. It should be noted that the situation is quite similar in materials science where most of the progress has been made on low-temperature mechanisms. It is only recently, driven by the problems of irradiation of nuclear materials and by the new possibilities of numerical modeling, that a renewed interest has been focused on climb.

The overview of the previous section shows that climb is needed both from the most recent experimental observations and from modeling of deep Earth minerals. Efforts to better document the activation of this mechanism, particularly in natural samples, must be continued and amplified. In planetary interiors, because pressure both inhibits dislocation glide and slows down diffusion, only climb offers a possibility for deforming high-pressure phases. A better understanding of this mechanism is needed, particularly in oxides and silicates with complex crystal chemistry.

As we have shown, numerical modeling offers new possibilities for studying climb and related high-temperature creep behavior, but this represents a challenging task, first because numerical modeling has to handle moving dislocations that are simultaneously sinks and sources for point defects. Whereas classical molecular dynamics simulations fail to capture the relevant timescale, the recent development of accelerated dynamics or the coupling of atomistic simulations with the KMC approach has shown their potentiality to tackle the problem of elementary dislocation climb processes and modeling of dislocation climb velocity. A major concern is nevertheless that, up to now, the modeling undertaken to simulate dislocation climb remains restricted to vacancy saturated conditions. At larger scales, the field of DD simulations has reached a point that gives insights on high-temperature phenomena. As an example, 2D DD simulations relying on the concept of glide and climb mobility law can be used to study the creep behavior. In particular, power-law creep of pure climb creep has been modeled using the 2D DD method, showing the possibility to extend our field of investigation. We have pointed out in the analysis of the microstructure in **Figure 9** that at the experimental strain rates, we see the recovery mechanisms operating, but the diffusion kinetics is not fast enough to counteract the hardening. The 2D DD modeling that describes the interplay between hardening and recovery allows us to explore the behavior at much lower strain rates by describing the operation of the same mechanisms. It predicts that diffusion-controlled recovery processes allow for steady-state deformation by dislocation creep in the lithospheric mantle. If reasonable stress levels (50–200 MPa) are considered, steady-state strain rates of 10^{-15}/s may be attained at temperatures as low as 900 K. Boioli et al. (2015b) showed that the predictions of this model are consistent with the strain rates observed in nature. This approach is also able, without the need of introducing any other mechanism, to reproduce a change from the power law to an exponential law (Gouriet et al. 2019), which is called the power-law breakdown (Goetze 1978). This change, which corresponds to a stronger dependence of the strain rate on stress, is observed for applied stresses above 200 MPa. Because the 2D DD model of creep is able, with only the activation of glide and climb, to reproduce this change of rheology, the use of two laws (power law at low stress and exponential law at high stress) to describe the creep of olivine appears not necessary from a theoretical point of view, and Gouriet et al. (2019) proposed using a single (exponential) low for the whole range of conditions of the upper mantle. More recently, an increasing number of 3D DD simulations with different schemes coupling diffusion and climb have been released. A clear tendency is to go beyond the concept of effective velocity by computing on the fly the climb velocity according to the point defect flux subjected to the condition that the defect concentration is in equilibrium and under the appropriate boundary conditions.

Another challenge is to consider the crystal chemistry complexity of minerals (oxides and silicates). Few studies have tackled this issue at the atomic scale (e.g., Zhai et al. 2020) compared to those carried out on metals. These materials can be sensitive to various parameters, such as the presence of aliovalent impurities or oxygen fugacity, which can induce, at least locally, deviations from stoichiometry. The effects of these parameters on high-temperature creep have been little studied, and exclusively on ceramics (e.g., Bretheau et al. 1979, Gaboriaud 1980), and with current numerical modeling capabilities they deserve increased attention.

Finally, it is worth stressing the importance of diffusion, which ultimately controls climb and therefore creep at high temperatures. Efforts to model climb are often hampered by a lack of (reliable) diffusion data. A major effort is required in this area, without which reliable modeling of the rheology of planetary interiors will not be possible. This effort needs to focus on the experimental side, where, in the case of high-pressure phases, the difficulty lies not only in the experimental conditions but also in the very sluggish diffusion. Efforts must also focus on modeling atomic-scale diffusion, which is difficult in minerals with complex crystallochemistry (multiple diffusion paths). The existence of several species with very different mobilities can have significant consequences. Jaoul (1980) showed very early on that the high-temperature deformation process is governed by an average of the diffusion properties of all the atomic components of the mineral and not only by the slowest diffusion species. Gaboriaud (1980) raised the question of possible local deviations from stoichiometry. These questions need to be investigated further.

DISCLOSURE STATEMENT

The authors are not aware of any affiliations, memberships, funding, or financial holdings that might be perceived as affecting the objectivity of this review.

ACKNOWLEDGMENTS

This project has received funding from the European Research Council under the European Union's Horizon 2020 research and innovation programme under grant agreement 787198, TimeMan.

LITERATURE CITED

Amelinckx S, Bontinck W, Maenhout-Van der Vorst W. 1957. Helical dislocations in CaF_2 and NaCl crystals. *Physica* 23:270–72. **https://doi.org/10.1016/S0031-8914(57)91947-X**

Amelinckx S, Strumane R. 1960. Geometry and kinetics of the polygonization of sodium chloride. *Acta Metall.* 8:312–20. **https://doi.org/10.1016/0001-6160(81)90156-5**

Argon AS, Moffatt WC. 1981. Climb of extended edge dislocations. *Acta Metall.* 29:293–99. **https://doi.org/10.1016/0001-6160(81)90156-5**

Ashby MF. 1972. A first report on deformation-mechanism maps. *Acta Metall.* 20:887–97. **https://doi.org/10.1016/0001-6160(72)90082-X**

Baker KL, Curtin WA. 2016. Multiscale diffusion method for simulations of long-time defect evolution with application to dislocation climb. *J. Mech. Phys. Solids* 92:297–312. **https://doi.org/10.1016/j.jmps.2016.04.006**

Ball A, White G. 1978. On the deformation of quartzite. *Phys. Chem. Miner.* 3:163–72. **https://doi.org/10.1007/BF00308119**

Ball A, Glover G. 1979. Dislocation climb deformation in quartz. *Bull. Minérol.* 102:188–94. **https://doi.org/10.3406/bulmi.1979.7275**

Ballufi RW. 1969. Mechanisms of dislocation climb. *Phys. Status Solidi* 31:443–63. **https://doi.org/10.1002/pssb.19690310202**

Barber DJ, Heard HC, Wenk HR. 1981. Deformation of dolomite single crystals from 20–800°C. *Phys. Chem. Miner.* 7:271–86. **https://doi.org/10.1007/BF00311980**

Barber DJ, Wenk HR, Gomez-Barreiro J, Rybacki E, Dresen G. 2007. Basal slip and texture development in calcite: new results from torsion experiments. *Phys. Chem. Miner.* 34:73–84. **https://doi.org/10.1007/s00269-006-0129-3**

Barr L, Hoodless I, Morrison J, Rudham R. 1960. Effects of gross imperfections on chloride ion diffusion in crystals of sodium chloride and potassium chloride. *Trans. Faraday Soc.* 56:697–708. **https://doi.org/10.1039/TF9605600697**

Bakó B, Groma I, Györgyi G, Zimányi G. 2006. Dislocation patterning: the role of climb in meso-scale simulations. *Comput. Mater. Sci.* 38:22–28. **https://doi.org/10.1016/j.commatsci.2005.12.034**

Bakó B, Clouet E, Dupuy LM, Blétry M. 2011. Dislocation dynamics simulations with climb: kinetics of dislocation loop coarsening controlled by bulk diffusion. *Philos. Mag.* 91:3173–91. **https://doi.org/10.1080/14786435.2011.573815**

Bardeen J, Herring C. 1952. Diffusion in alloys and the Kirkendall effect. In *Imperfections in Nearly Perfect Crystals*, ed. W Schockley, pp. 261–88. New York: Wiley

Ben Ismaïl W, Mainprice D. 1998. An olivine fabric database: an overview of upper mantle fabrics and seismic anisotropy. *Tectonophysics* 296:145–57. **https://doi.org/10.1016/S0040-1951(98)00141-3**

Bestmann M, Prior DJ. 2003. Intragranular dynamic recrystallization in naturally deformed calcite marble: diffusion accommodated grain boundary sliding as a result of subgrain rotation recrystallization. *J. Struct. Geol.* 25:1597–613. **https://doi.org/10.1016/S0191-8141(03)00006-3**

Boioli F, Carrez P, Cordier P, Devincre B, Marquille M. 2015a. Modeling the creep properties of olivine by 2.5-dimensional dislocation dynamics simulations. *Phys. Rev. B* 92:014115. **https://doi.org/10.1103/PhysRevB.92.014115**

Boioli F, Tommasi A, Cordier P, Demouchy S, Mussi A. 2015b. Low steady-state stresses in the cold lithospheric mantle inferred from dislocation dynamics models of dislocation creep in olivine. *Earth Planet. Sci. Lett.* 432:232–42. **https://doi.org/10.1016/j.epsl.2015.10.012**

Boioli F, Carrez P, Cordier P, Devincre B, Gouriet K, et al. 2017. Pure climb creep mechanism drives flow in the Earth's lower mantle. *Sci. Adv.* 3:e1601958. **https://doi.org/10.1126/sciadv.1601958**

Braillon P, Kubin L, Serughetti J. 1978. Plastic deformation of calcite single crystals deformed in compression parallel to [111]. *Phys. Status Solidi (a)* 45:453–62. **https://doi.org/10.1002/pssa.2210450212**

Bretheau T, Castaing J, Rabier J, Veyssière P. 1979. Mouvement des dislocations et plasticité à haute temperature des oxydes binaires et ternaires. *Adv. Phys.* 28:835–1014. **https://doi.org/10.1080/00018737900101465**

Brunner D, Taeri-Baghbadrani S, Sigle W, Rühle M. 2001. Surprising results of a study on the plasticity in strontium titanate. *J. Am. Ceram. Soc.* 84:1161–63. **https://doi.org/10.1111/j.1151-2916.2001.tb00805.x**

Caillard D, Martin JL. 2003. *Thermally Activated Mechanisms in Crystal Plasticity*. Oxford, UK: Elsevier

Caillard D, Vanderschaeve G, Bresson L, Gratias D. 2000. Transmission electron microscopy study of dislocations and extended defects in as-grown icosahedral Al-Pd-Mn single grains. *Philos. Mag. A* 80:237–53. **https://doi.org/10.1080/01418610008212051**

Caillard D, Roucau C, Bresson L, Gratias D. 2002. Dislocation motions in 5-fold planes of icosahedral Al-Pd-Mn. *Acta Mater.* 50:4499–509. **https://doi.org/10.1016/S1359-6454(02)00268-9**

Carrez P, Cordier P. 2017. Plastic deformation of materials under pressure. *MRS Bull.* 42:714–17. **https://doi.org/10.1557/mrs.2017.213**

Carrez P, Ferré D, Denoual C, Cordier P. 2010. Modelling thermal activation of <110>{110} slip at low temperature in $SrTiO_3$. *Scr. Mater.* 63:434–37. **https://doi.org/10.1016/j.scriptamat.2010.04.045**

Castelnau O, Derrien K, Ritterbex S, Carrez P, Cordier P, Moulinec H. 2020. Multiscale modeling of the effective viscoplastic behavior of Mg_2SiO_4 wadsleyite: bridging atomic and polycrystal scales. *C. R. Méc.* 348:827–46. **https://doi.org/10.5802/crmeca.61**

Cherns D, Hirsch P, Saka H. 1980. Mechanism of climb of dissociated dislocations. *Proc. R. Soc. A* 371:213–34. **https://doi.org/10.1098/rspa.1980.0077**

Chien FR, Heuer AH. 1996. Lattice diffusion kinetics in Y_2O_3-stabilized cubic ZrO_2 single crystals: a dislocation loop annealing study. *Philos. Mag. A* 73:681–97. **https://doi.org/10.1080/01418619608242990**

Cordier C, Doukhan JC. 1989. Water solubility in quartz and its influence on ductility. *Eur. J. Mineral.* 1:221–37. **https://doi.org/10.1127/ejm/1/2/0221**

Cordier P, Gouriet K, Weidner T, Van Orman J, Castelnau O, et al. 2023. Periclase deforms slower than bridgmanite under mantle conditions. *Nature* 613:303–7. **https://doi.org/10.1038/s41586-022-05410-9**

Couret A. 2010. Low and high temperature deformation mechanisms in TiAl alloys. *J. Phys. Conf. Ser.* 240:012001. **https://doi.org/10.1088/1742-6596/240/1/012001**

Demouchy S, Tommasi A, Boffa Ballaran T, Cordier P. 2013. Low strength of Earth's uppermost mantle inferred from tri-axial deformation experiments on dry olivine crystals. *Phys. Earth Planet. Inter.* 220:37–49. **https://doi.org/10.1016/j.pepi.2013.04.008**

Demouchy S, Mussi A, Barou F, Tommasi A, Cordier P. 2014. Viscoplasticity of polycrystalline olivine experimentally deformed at high pressure and 900°C. *Tectonophysics* 623:123–35. **https://doi.org/10.1016/j.tecto.2014.03.022**

Demouchy S, Mussi A, Weidner T, Gardés E, Cordier P. 2024. Dislocations in naturally deformed olivine: example of a mylonitic peridotite. *Phys. Earth Planet. Inter.* 346:107125. **https://doi.org/10.1016/j.pepi.2023.107125**

Douin J, Beauchamp P, Veyssière P. 1988. Climb dissociation on {310} planes in nearly-stoichiometric Ni_3Al. *Philos. Mag. A* 58:923–35. **https://doi.org/10.1080/01418618808214423**

Doukhan N, Duclos R, Escaig B. 1982. Climb dissociation in {113} planes in Al-Mg spinel. *J. Phys.* 43:1149–57. **https://doi.org/10.1051/jphys:019820043070114900**

Donlon WT, Mitchell TE, Heuer AH. 1979. Climb dissociation of network dislocations in non–stoichiometric Mg–Al spinel. *Philos. Mag. A* 40:351–66. **https://doi.org/10.1080/01418617908234845**

Donlon WT, Heuer AH, Mitchell TE. 1998. Compositional softening in Mg-A1 spinel. *Philos. Mag. A* 78:615–41. **https://doi.org/10.1080/01418619808241926**

Dorn JE. 1954. Some fundamental experiments on high temperature creep. *J. Mech. Phys. Solids* 8:85–116. **https://doi.org/10.1016/0022-5096(55)90054-5**

Durham WB, Goetze G. 1977. Plastic flow of oriented single crystals of olivine. 1. Mechanical data. *J. Geophys. Res.* 82(36):5737–53. **https://doi.org/10.1029/JB082i036p05737**

Edelin G, Levy V. 1973. Observation de sources de Bardeen-Herring dans le magnesium trempé. *Philos. Mag. A* 27:487–97. **https://doi.org/10.1080/14786437308227423**

Edelin G, Poirier JP. 1973a. Etude de la montée des dislocations au moyen d'expériences de fluage par diffusion dans le magnesium. I. Mécanismes de déformation. *Philos. Mag.* 28:1203–10. **https://doi.org/10.1080/14786437308227994**

Edelin G, Poirier JP. 1973b. Etude de la montée des dislocations au moyen d'expériences de fluage par diffusion dans le magnesium. II. Mesure de la vitesse de montée. *Philos. Mag.* 28:1211–23. **https://doi.org/10.1080/14786437308227995**

Epishin A, Link T. 2004. Mechanisms of high temperature creep of nickel-base superalloys under low applied stress. *Philos. Mag.* 84:1979–2000. **https://doi.org/10.1080/14786430410001663240**

Escaig B. 1963. Emission et absorption de défauts ponctuels par les dislocations dissociées. *Acta Metall.* 11:595–610. **https://doi.org/10.1016/0001-6160(63)90094-4**

Evans DJ, Scheltens FJ, Woodhouse JB, Fraser HL. 1997. Deformation mechanisms in $MoSi_2$ at temperatures above the brittle-to-ductile transition temperature I. Polycrystalline $MoSi_2$. *Philos. Mag. A* 75:1–15. **https://doi.org/10.1080/01418619708210278**

Feng Z, Fu R, Lin C, Wu G, Huang T, et al. 2020. TEM-based dislocation tomography: challenges and opportunities. *Curr. Opin. Solid State Mater. Sci.* 24:100833. **https://doi.org/10.1016/j.cossms.2020.100833**

Firestone RF, Heuer AH. 1976. Creep deformation of 0° sapphire. *J. Am. Ceram. Soc.* 59:24–29. **https://doi.org/10.1111/j.1151-2916.1976.tb09379.x**

Friedel J. 1964. *Dislocations*. Oxford, UK: Pergamon

Gaboriaud RJ. 1980. Climb model of dislocations in oxides. *J. Mater. Sci.* 15:2091–96. **https://doi.org/10.1007/BF00550636**

Gaboriaud RJ. 1981. Fluage haute temperature du sesquioxyde d'yttrium: Y_2O_3. *Philos. Mag. A* 44:561–87. **https://doi.org/10.1080/01418618108236162**

Galy B, Musi M, Hantcherli M, Molénat G, Couret A, et al. 2023. Glide and mixed climb dislocation velocity in γ-TiAl investigated by in-situ transmission electron microscopy. *Scr. Mater.* 228:115333. **https://doi.org/10.1016/j.scriptamat.2023.115333**

Gao Y, Zhuang Z, Liu ZL, You XC, Zhao XC, Zhang ZH. 2011. Investigations of pipe-diffusion-based dislocation climb by discrete dislocation dynamics. *Int. J. Plast.* 27:1055–71. **https://doi.org/10.1016/j.ijplas.2010.11.003**

Goetze C, Kohlstedt DL. 1973. Laboratory study of dislocation climb and diffusion in olivine. *J. Geophys. Res.* 78(26):5961–71. **https://doi.org/10.1029/JB078i026p05961**

Goetze C. 1978. The mechanisms of creep in olivine. *Philos. Trans. R. Soc. A* 288:99–119. **http://doi.org/10.1098/rsta.1978.0008**

Gouriet K, Cordier P, Garel F, Thoraval C, Demouchy S, et al. 2019. Dislocation dynamics modelling of the power-law breakdown in olivine single crystals: toward a unified creep law for the upper mantle. *Earth Planet. Sci. Lett.* 506:282–91. **https://doi.org/10.1016/j.epsl.2018.10.049**

Gratias D, Beauchesne JT, Mompiou F, Caillard D. 2006. Geometry of dislocations in icosahedral quasicrystals. *Philos. Mag.* 86:4139–51. **https://doi.org/10.1080/14786430600575435**

Green H II. 1976. Plasticity of olivine in peridotites. In *Electron Microscopy in Mineralogy*, ed. HR Wenk, pp. 443–64. Berlin: Springer. **https://doi.org/10.1007/978-3-642-66196-9_34**

Green HW II, Radcliffe SV. 1972. Deformation processes in the upper mantle. In *Flow and Fracture of Rocks*, Vol. 16, ed. HC Heard, IY Barg, NL Carter, CB Raleigh, pp. 139–56. Washington, DC: Am. Geophys. Union. **https://doi.org/10.1029/GM016p0139**

Grilhé J, Boisson M, Seshan K, Gaboriaud RJ. 1977. Climb model of extended dislocations in f.c.c. metals. *Philos. Mag.* 36:923–30. **https://doi.org/10.1080/14786437708239767**

Groves GW, Kelly A. 1969. Change of shape due to dislocation climb. *Philos. Mag.* 19:977–86. **https://doi.org/10.1080/14786436908225862**

Gu Y, Xiang Y, Srolovitz DJ. 2016. Relaxation of low-angle grain boundary structure by climb of the constituent dislocations. *Scripta Mater.* 114:35–40. **https://doi.org/10.1016/j.scriptamat.2015.11.016**

Gu Y, Xiang Y, Srolovitz DJ, El-Awady JA. 2018. Self-healing of low angle grain boundaries by vacancy diffusion and dislocation climb. *Scripta Mater.* 155:155–59. **https://doi.org/10.1016/j.scriptamat.2018.06.035**

Gumbsch P, Taeri-Baghbadrani S, Brunner D, Sigle W, Rühle M. 2001. Plasticity and an inverse brittle-to-ductile transition in strontium titanate. *Phys. Rev. Lett.* 87:085505. **https://doi.org/10.1103/PhysRevLett.87.085505**

Hawemann F, Mancktelow N, Wex S, Pennacchioni G, Camacho A. 2019. Fracturing and crystal plastic behavior of garnet under seismic stress in the dry lower continental crust (Musgrave Ranges, Central Australia). *Solid Earth* 10:1635–49. **https://doi.org/10.5194/se-10-1635-2019**

Hentschel F, Trepmann CA, Janots E. 2019. Deformation of feldspar at greenschist facies conditions—the record of mylonitic pegmatites from the Pfunderer Mountains, Eastern Alps. *Solid Earth* 10:95–116. **https://doi.org/10.5194/se-10-95-2019**

Hirel P, Carrez P, Cordier P. 2016. From glissile to sessile: effect of temperature on <110>dislocations in perovskite materials. *Scr. Mater.* 120:67–70. **https://doi.org/10.1016/j.scriptamat.2016.04.001**

Hirel P, Kraych A, Carrez P, Cordier P. 2014. Atomic core structure and mobility of [100](010) and [010](100) dislocations in $MgSiO_3$ perovskite. *Acta Mat.* 79:117–25. **https://doi.org/10.1016/j.actamat.2014.07.001**

Hirsch PB, Silcox J, Smallman RE, Westmacott KH. 1958. Dislocation loops in quenched aluminium. *Philos. Mag.* 3:897–908. **https://doi.org/10.1080/14786435808237028**

Hirsch PB. 1962. Extended jogs in dislocations in face-centred cubic metals. *Philos. Mag.* 7:67:93. **https://doi.org/10.1080/14786436208201859**

Hwang SL, Shen P, Yui TF, Chu HT. 2003. On the mechanism of resorption zoning in metamorphic garnet. *J. Metamorph. Geol.* 21:761–69. **https://doi.org/10.1046/j.1525-1314.2003.00477.x**

Jaoul O. 1980. Multicomponent diffusion and creep in olivine. *J. Geophys. Res.* 95(B11):17631–42. **https://doi.org/10.1029/JB095iB11p17631**

Ji S, Martignole J. 1994. Ductility of garnet as an indicator of extremely high temperature deformation. *J. Struct. Geol.* 16:985–96. **https://doi-org.ressources-electroniques.univ-lille.fr/10.1016/0191-8141(94)90080-9**

Junqua N, Grilhé J. 1984. Apparition d'instabilités sur des dipoles de dislocations coin. *Acta Metall.* 32:2139–47. **https://doi.org/10.1016/0001-6160(84)90157-3**

Kabir M, Lau TT, Rodney D, Yip S, Van Vliet KJ. 2010. Predicting dislocation climb and creep from explicit atomistic details. *Phys. Rev. Lett.* 105:095501. **https://doi.org/10.1103/PhysRevLett.105.095501**

Kad BK, Fraser HL. 1994. On the contribution of climb to high-temperature deformation in single phase γ-TiAl. *Philos. Mag. A* 69:689–99. **https://doi.org/10.1080/01418619408242511**

Keralavarma SM, Cagin T, Arsenlis A, Benzerga AA. 2012. Power-law creep from discrete dislocation dynamics. *Phys. Rev. Lett.* 109:265504. **https://doi.org/10.1103/PhysRevLett.109.265504**

Kirby SH, Raleigh CB. 1973. Mechanisms of high-temperature, solid-state flow in minerals and ceramics and their bearing on the creep behavior of the mantle. *Tectonophysics* 19:165–94. **https://doi.org/10.1016/0040-1951(73)90038-3**

Kirby SH, Wegner MW. 1978. Dislocation substructure of mantle-derived olivine as revealed by selective chemical etching and transmission electron microscopy. *Phys. Chem. Miner.* 3:309–30. **https://doi.org/10.1007/BF00311845**

Kohnert AA, Capolungo L. 2022. The kinetics of static recovery by dislocation climb. *NPJ Comput. Mater.* 8:104. **https://doi.org/10.1038/s41524-022-00790-y**

Lagerlöf KPD, Mitchell TE, Heuer AH. 1989. Energetics of the break-up of dislocation dipoles into prismatic loops. *Acta Metall.* 37:3315–25. **https://doi.org/10.1016/0001-6160(89)90204-6**

Landeiro Dos Reis ML, Giret Y, Carrez P, Cordier P. 2022. Efficiency of the vacancy pipe diffusion along an edge dislocation in MgO. *Comput. Mater. Sci.* 211:111490. **https://doi.org/10.1016/j.commatsci.2022.111490**

Lau TT, Lin X, Yip S, Van Vliet KJ. 2009. Atomistic examination of the unit processes and vacancy-dislocation interaction in dislocation climb. *Scripta Mater.* 60:399–402. **https://doi.org/10.1016/j.scriptamat.2008.11.019**

Legros M, Dehm G, Artz E, Balk J. 2008. Observation of giant diffusivity along dislocation cores. *Science* 319:1646–49. **https://doi.org/10.1126/science.1151771**

Le Hazif R, Edelin G, Dupouy JM. 1973. Diffusion creep by dislocation climb in beryllium and Be-Cu single crystals. *Metall. Trans.* 4:1275–81. **https://doi.org/10.1007/BF02644522**

Lin D, Wang Y, Liu J, Law CC. 1999. Brittle-to-ductile transition temperature and its controlling mechanism in Ti-47Al-2Mn-2Nb alloy. *J. Chin. Inst. Eng.* 22:55–60. **https://doi.org/10.1080/02533839.1999.9670441**

Liu F, Liu Z, Lin P, Zhuang Z. 2017. Numerical investigations of helical dislocations based on coupled glide-climb model. *Int. J. Plast.* 92:2–18. **https://doi.org/10.1016/j.ijplas.2017.02.015**

Liu F, Cocks ACF, Gill SPA, Tartelon E. 2020. An improved method to model dislocation self-climb. *Model. Simul. Mater. Sci. Eng.* 28:055012. **https://doi.org/10.1088/1361-651X/ab81a8**

Lothe J. 1960. Theory of dislocation climb in metals. *J. Appl. Phys.* 31:1077–87. **https://doi.org/10.1063/1.1735749**

Malaplate J, Caillard D, Couret A. 2004. Interpretation of the stress dependence of creep by a mixed climb mechanism in TiAl. *Philos. Mag.* 84:3671–87. **https://doi.org/10.1080/14786430412331284009**

Martelat JE, Malamoud K, Cordier P, Randrianasolo B, Schulmann K, Lardeaux JM. 2012. Garnet crystal plasticity in the continental crust, new example from south Madagascar. *J. Metamorph. Geol.* 30:435–52. **https://doi.org/10.1111/j.1525-1314.2012.00974.x**

Matthews JW, Klokholm E, Plaskett TS, Sadagopan S. 1973. Helical dislocations in gadolinium gallium garnet ($Gd_3Ga_5O_{12}$). *Phys. Status Solidi (a)* 19:671–78. **https://doi.org/10.1002/pssa.2210190233**

McElfresh C, Cui Y, Dudarev SL, Po G, Marian J. 2021. Discrete stochastic model of point defect-dislocation interaction for simulating dislocation climb. *Int. J. Plast.* 136:102848. **https://doi.org/10.1016/j.ijplas.2020.102848**

McLaren AC, Fitz Gerald JD, Gerretsen J. 1989. Dislocation nucleation and multiplication in synthetic quartz: relevance to water weakening. *Phys. Chem. Minerals* 16:465–82. **https://doi.org/10.1007/BF00197016**

Minster JB, Anderson DL. 1980. Dislocations and nonelastic processes in the mantle. *J. Geophys. Res.* 85(B11):6347–52. **https://doi.org/10.1029/JB085iB11p06347**

Mompiou F, Bresson L, Cordier P, Caillard D. 2003. Dislocation-climb and low-temperature plasticity of an Al-Pd-Mn quasicrystal. *Philos. Mag.* 83:3133–57. **https://doi.org/10.1080/1478643031000155110**

Mompiou F, Caillard D, Feuerbacher M. 2004. In-situ observation of dislocation motion in icosahedral Al–Pd–Mn quasicrystals. *Philos. Mag.* 84:2777–92. **https://doi.org/10.1080/14786430410001671494**

Mompiou F, Caillard D. 2008a. On the stress exponent of dislocation climb velocity. *Mater. Sci. Eng. A* 483–484:143–47. **https://doi.org/10.1016/j.msea.2006.12.166**

Mompiou F, Caillard D. 2008b. Dislocation-climb plasticity: modelling and comparison with the mechanical properties of icosahedral AlPdMn. *Acta Mater.* 56:2262–71. **https://doi.org/10.1016/j.actamat.2008.01.015**

Mompiou F, Caillard D. 2014. Dislocation and mechanical properties of icosahedral quasicrystals. *C. R. Phys.* 15:82–89. **https://doi.org/10.1016/j.crhy.2013.09.003**

Morales LFG, Mainprice D, Lloyd GE, Law RD. 2011. Crystal fabric development and slip systems in a quartz mylonite: an approach via transmission electron microscopy and viscoplastic self-consistent modelling. *Geol. Soc. Lond. Spec. Publ.* 360:151–74. **https://doi.org/10.1144/SP360.9**

Mordehai D, Clouet E, Fivel M, Verdier M. 2008. Introducing dislocation climb by bulk diffusion in discrete dislocation dynamics. *Philos. Mag.* 88:899–925. **https://doi.org/10.1080/14786430801992850**

Mott NF. 1951. The mechanical properties of metals. *Proc. Phys. Soc. B* 64:729–41. **https://doi.org/10.1088/0370-1301/64/9/301**

Mott NF. 1953. Bakerian lecture: dislocations, plastic flow and creep. *Proc. R. Soc. A* 220:1–14. **https://doi.org/10.1098/rspa.1953.0167**

Muramoto M, Michibayashi K, Ando J-I, Kagi H. 2011. Rheological contrast between garnet and clinopyroxene in the mantle wedge: an example from Higashi-akaishi peridotite mass, SW Japan. *Phys. Earth Planet. Sci.* 184:14–33. **https://doi.org/10.1016/j.pepi.2010.10.008**

Mussi A, Cordier P, Frost D. 2013. Transmission electron microscopy characterization of the dislocations and slip systems of the dense hydrous magnesium silicate superhydrous B. *Eur. J. Mineral.* 25:561–68. **https://doi.org/10.1127/0935-1221/2013/0025-2308**

Mussi A, Carrez P, Gouriet K, Hue B, Cordier P. 2021a. 4D electron tomography of dislocations undergoing electron irradiation. *C. R. Phys.* 22:67–81. **https://doi.org/10.5802/crphys.80**

Mussi A, Gallet J, Castelnau O, Cordier P. 2021b. Application of electron tomography of dislocations in beam-sensitive quartz to the determination of strain components. *Tectonophysics* 803:228754. **https://doi.org/10.1016/j.tecto.2021.228754**

Naanani S, Monchoux JP, Mabru C, Couret A. 2018. Pure climb of [001]dislocations in TiAl at 850°C. *Scr. Mater.* 149:53–57. **https://doi.org/10.1016/j.scriptamat.2018.02.002**

Nabarro FRN. 1967a. *Theory of Crystal Dislocations*. Oxford, UK: Clarendon

Nabarro FRN. 1967b. Steady-state diffusional creep. *Philos. Mag.* 16:231–37. **https://doi.org/10.1080/14786436708229736**

Phakey P, Dollinger G, Christie J. 1972. Transmission electron microscopy of experimentally deformed olivine crystals. In *Flow and Fracture of Rocks*, Vol. 16, ed. HC Heard, IY Barg, NL Carter, CB Raleigh, pp. 117–38. Washington, DC: Am. Geophys. Union. **https://doi.org/10.1029/GM016p0117**

Phillips DS, Mitchell TE, Heuer AH. 1982a. Climb dissociation of dislocations in sapphire (α-Al_2O_3) revisited: crystallography of dislocation dipoles. *Philos. Mag.* 45:371–85. **https://doi.org/10.1080/01418618208236177**

Phillips DS, Pletka BJ, Heuer A, Mitchell TE. 1982b. An improved model of break-up of dislocation dipoles into loops: application to sapphire (α-Al_2O_3). *Acta Metall.* 30:491–98. **https://doi.org/10.1016/0001-6160(82)90229-2**

Pletka BJ, Mitchell TE, Heuer A. 1982. Dislocation substructures in doped sapphire (α-Al_2O_3) deformed by basal slip. *Acta Metall.* 30:147–56. **https://doi.org/10.1016/0001-6160(82)90054-2**

Prior DJ, Wheeler J, Brenker FE, Harte B, Matthews M. 2000. Crystal plasticity of natural garnet: new microstructural evidence. *Geology* 28:1003–6. **https://doi.org/10.1130/0091-7613(2000)28<1003:CPONGN>2.0.CO;2**

Raleigh CB, Kirby SH. 1970. Creep in the upper mantle. *Mineral. Soc. Am. Spec. Pap.* 3:113–21

Reali R, Van Orman J, Pigott J, Jackson JM, Boioli F, et al. 2019. The role of diffusion-driven pure climb creep on the rheology of bridgmanite under lower mantle conditions. *Sci. Rep.* 9:2053. **https://doi.org/10.1038/s41598-018-38449-8**

Reiner M. 1964. The Deborah number. *Phys. Today* 17:62. **https://doi.org/10.1063/1.3051374**

Ritterbex S, Carrez P, Gouriet K, Cordier P. 2015. Modeling dislocation glide in Mg_2SiO_4 ringwoodite: towards rheology under transition zone conditions. *Phys. Earth Planet. Inter.* 248:20–29. **https://doi.org/10.1016/j.pepi.2015.09.001**

Ritterbex S, Carrez P, Cordier P. 2016. Modeling dislocation glide and lattice friction in Mg_2SiO_4 wadsleyite in conditions of the Earth's transition zone. *Am. Mineral.* 101:2085–94. **https://doi.org/10.2138/am-2016-5578CCBYNCND**

Ritterbex S, Carrez P, Cordier P. 2020. Deformation across the mantle transition zone: a theoretical mineral physics view. *Earth Planet. Sci. Lett.* 547:116438. **https://doi.org/10.1016/j.epsl.2020.116438**

Sarkar S, Li J, Cox WT, Bitzek E, Lenosky TJ, Wang Y. 2012. Finding activation pathway of coupled displacive-diffusional defect processes in atomistics: dislocation climb in fcc copper. *Phys. Rev. B* 86:014115. **https://doi.org/10.1103/PhysRevB.86.014115**

Seitz F. 1950. The generation of vacancies by dislocations. *Phys. Rev.* 79:1002–3. **https://doi.org/10.1103/PhysRev.79.1002.2**

Sigle W, Sarbu C, Brunner D, Rühle M. 2006. Dislocations in plastically deformed $SrTiO_3$. *Philos. Mag.* 86:4809–21. **https://doi.org/10.1080/14786430600672695**

Silcox J, Whelan MJ. 1960. Direct observations of the annealing of prismatic dislocation loops and of climb of dislocations in quenched aluminium. *Philos. Mag.* 5:1–23. **https://doi.org/10.1080/14786436008241196**

Skrotzki W. 1992. Defect structure and deformation mechanisms in naturally deformed hornblende. *Phys. Stat. Sol. (a)* 131:605–24

Stroh AN. 1954. Constrictions and jogs in extended dislocations. *Proc. Phys. Soc. B* 67:427–36. **https://doi.org/10.1088/0370-1301/67/5/307**

Swinburne TD, Arakawa K, Mori H, Yasuda H, Isshiki M, et al. 2016. Fast, vacancy-free climb of prismatic dislocation loops in bcc metals. *Sci. Rep.* 6:30596. **https://doi.org/10.1038/srep30596**

Tang X, Lagerlöf KPD, Heuer AH. 2003. Determination of pipe diffusion coefficients in undoped and magnesia-doped sapphire (α-Al_2O_3): a study based on annihilation of dislocation dipoles. *J. Am. Ceram. Soc.* 86:560–65. **https://doi.org/10.1111/j.1151-2916.2003.tb03341.x**

Thomson RM, Balluffi RW. 1962. Kinetic theory of dislocation climb. I. General models for edge and screw dislocations. *J. Appl. Phys.* 33:803–16

Tisone TC, Marshall GW, Brittain JO. 1968. Prismatic dislocations in β' NiAl. *J. Appl. Phys.* 39:3714–17. **https://doi.org/10.1063/1.1656845**

Tullis J, Yund R. 1989. Hydrolytic weakening of quartz aggregates: the effects of water and pressure on recovery. *Geophys. Res. Lett.* 16:1343–46. **https://doi.org/10.1029/GL016i011p01343**

Tullis J, Yund R. 1992. The Brittle-ductile transition in feldspar aggregates: an experimental study. *Int. Geophys.* 51:89–117. **https://doi.org/10.1016/S0074-6142(08)62816-8**

Van Orman J, Crispin K. 2010. Diffusion in oxides. *Rev. Mineral. Geochem.* 72:757–825. **https://doi.org/10.2109/jcersj1950.74.851_215**

Veyssière P, Grilhé J. 1971. Experimental study of the influence of some parameters on the helical dislocations equilibrium in quenched alloys. *Acta Metall.* 19:1047–51. **https://doi.org/10.1016/0001-6160(71)90037-X**

Veyssière P, Rabier J, Garem GJ. 1976. Sous-joints de dislocations et dissociations dans le ferrite de nickel déformé plastiquement à 0,85 T_F. *Philos. Mag.* 33:143–63. **https://doi.org/10.1080/14786437608221099**

Veyssière P, Rabier J, Garem GJ. 1978. Influence of temperature on dissociation of dislocations and plastic deformation in spinel oxides. *Philos. Mag.* 38:61–79. **https://doi.org/10.1080/01418617808239218**

Voegelé V, Cordier P, Sautter V, Sharp TG, Lardeaux JM, Marques FO. 1998. Plastic deformation of silicate garnets. II. Deformation microstructures in natural samples. *Phys. Earth Planet. Inter.* 108:319–38. **https://doi.org/10.1016/S0031-9201(98)00111-3**

Voisin T, Monchoux JP, Thomas M, Deshayes C, Couret A. 2016. Mechanical properties of the TiAl IRIS alloy. *Metall. Mater. Trans. A* 47:6097–108. **https://doi.org/10.1007/s11661-016-3801-3**

Weertman J. 1955. Theory of steady-state creep based on dislocation climb. *J. Appl. Phys.* 26:1213–17. **https://doi.org/10.1063/1.1721875**

Weertman J. 1957. Helical dislocations. *Phys. Rev.* 107:1259–61. **https://doi.org/10.1103/PhysRev.107.1259**

Weertman J. 1970. The creep strength of the Earth's mantle. *Rev. Geophys. Space Phys.* 8:145–68. **https://doi.org/10.1029/RG008i001p00145**

Westmacott KH, Barnes RS, Smallman RE. 1962. The observation of a dislocation 'climb' source. *Philos. Mag.* 7:1585–96. **https://doi.org/10.1080/14786436208213293**

White S. 1975. Tectonic deformation and recrystallisation of oligoclase. *Contrib. Mineral. Petrol.* 50:287–304. **https://doi.org/10.1007/BF00394854**

White S. 1977. Geological significance of recovery and recrystallization processes in quartz. *Tectonophysics* 39:143–70. **https://doi.org/10.1016/0040-1951(77)90093-2**

Willaime C, Christie JM, Kovacs MP. 1979. Experimental deformation of K-feldspar single crystals. *Bull. Minéral.* 102:168–77. **https://doi.org/10.3406/bulmi.1979.7272**

Wollgarten M, Bartschs M, Messerschmidt U, Feuerbacher M, Rosenfeld R, et al. 1995. In-situ observation of dislocation motion in icosahedral Al-Pd-Mn single quasicrystals. *Philos. Mag. Lett.* 71:99–105. **https://doi.org/10.1080/09500839508241001**

Yang M, Flynn C. 1994. Intrinsic diffusion properties of an oxide: MgO. *Phys. Rev. Lett.* 73:1809–12. **https://doi.org/10.1103/PhysRevLett.73.1809**

Yi J, Argon AS, Sayir A. 2006. Internal stresses and the creep resistance of the directionally solidified ceramic eutectics. *Mater. Sci. Eng. A* 421:86–102. **https://doi.org/10.1016/j.msea.2005.10.012**

Zhai JH, Hirel P, Carrez P. 2020. Atomic-scale properties of jogs along 1/2 <110>{$\bar{1}$10} edge dislocations in MgO. *Scripta Mater*. 181:66–69. **https://doi.org/10.1016/j.scriptamat.2020.02.013**

Zhang Z, Sigle W, Kurtz W, Rühle M. 2002. Electronic and atomic structure of a dissociated dislocation in $SrTiO_3$. *Phys. Rev. B* 66:214112. **https://doi.org/10.1103/PhysRevB.66.214112**

Zheng JG, Li Q, Feng D. 1993. Climb dissociation of |*c*| dislocations in Y-Ba-Cu-O superconductors. *Mater. Sci. Forum* 129:147–54. **https://doi.org/10.4028/www.scientific.net/MSF.129.147**